Dynamic population stage structure due to juvenile–adult asymmetry stabilizes complex ecological communities

André M. de Roos[a,b,1]

[a]Institute for Biodiversity and Ecosystem Dynamics, University of Amsterdam, 1090 GE Amsterdam, The Netherlands; and [b]Santa Fe Institute, Santa Fe, NM 87501

Edited by Simon Asher Levin, Princeton University, Princeton, NJ, and approved April 12, 2021 (received for review November 15, 2020)

Natural ecological communities are diverse, complex, and often surprisingly stable, but the mechanisms underlying their stability remain a theoretical enigma. Interactions such as competition and predation presumably structure communities, yet theory predicts that complex communities are stable only when species growth rates are mostly limited by intraspecific self-regulation rather than by interactions with resources, competitors, and predators. Current theory, however, considers only the network topology of population-level interactions between species and ignores within-population differences, such as between juvenile and adult individuals. Here, using model simulations and analysis, I show that including commonly observed differences in vulnerability to predation and foraging efficiency between juvenile and adult individuals results in up to 10 times larger, more complex communities than observed in simulations without population stage structure. These diverse communities are stable or fluctuate with limited amplitude, although in the model only a single basal species is self-regulated, and the population-level interaction network is highly connected. Analysis of the species interaction matrix predicts the simulated communities to be unstable but for the interaction with the population-structure subsystem, which completely cancels out these instabilities through dynamic changes in population stage structure. Common differences between juveniles and adults and fluctuations in their relative abundance may hence have a decisive influence on the stability of complex natural communities and their vulnerability when environmental conditions change. To explain community persistence, it may not be sufficient to consider only the network of interactions between the constituting species.

food webs | community dynamics | community complexity | population stage structure | resilience

Ecological communities have traditionally been conceptualized as collections of species that are connected with each other through a network of positive and negative interactions. This species-based paradigm adopts the population as the fundamental unit of measurement or modeling, altogether ignores differences between individuals within populations, and hence considers the vital rates of all conspecific individuals to be identical. Yet, it is individuals, not species, that interact. Furthermore, in real populations no two individuals are alike, mostly because of differences in their developmental stage (1). And vital rates are definitely not the same for all individuals as only juveniles grow and mature, while only adults reproduce. This raises the question of to what extent current theoretical insights about dynamics of ecological communities are robust or, alternatively, are artifacts of the species-level scale of study of ecological communities (2).

One of the core elements of the theory about ecological community dynamics pertains to the relationship between community complexity, diversity, and stability, which has been explored at length through dynamic simulations of the network of species interactions (3, 4) or through analysis of the community matrix (5), the elements of which measure how strongly the species in a community affect each other's growth rate. Using community matrices, Robert May (6, 7) theoretically predicted almost half a century ago that large, complex ecological communities are less stable than simpler ones, refuting prevailing ideas that complexity begets stability (8, 9). He challenged ecologists to "…elucidate the devious strategies which make for stability in enduring natural systems" (p. 174 in ref. 7). May's findings initiated the diversity–stability debate in ecology (10) and the search for special characteristics and constraints on natural communities promoting stability (11). Analysis of different types of community matrices (12) has uncovered a range of mechanisms that benefit community stability, such as weak interaction strength (13); adaptive foraging (14); allometric scaling of interaction strength (15); and omnivorous (16), mutualistic (17), or high-order interactions (18). The diversity–stability conundrum seems, however, far from resolved, given that a recent review concluded that for community stability to occur "at least half—and possibly more than 90%—of species must be subject to self-regulation to a substantial degree" (p. 1873 in ref. 19), even though clear empirical evidence for self-regulation is lacking and the extent to which it occurs in natural populations is debated (16, 20–22). Paradoxically therefore, while competitive and predatory interactions between species are considered the two most important, structuring forces of ecological communities (23), direct, negative effects of species on their own growth rate seem crucial for community stability (19).

The network of population-level interactions between species in the community, its topology, the nature of these interactions,

Significance

Using food web models that account for juvenile and adult individuals of species, I show that commonly observed differences between juveniles and adults in foraging capacity and predation risk result in larger, more complex communities than predicted by models without stage structure. Based on their species interaction networks these complex and diverse communities would be expected to be unstable, but these destabilizing effects of species interactions are overruled by stabilizing changes in juvenile–adult stage structure. Differences between juvenile and adult individuals hence offer a natural resolution to the diversity–stability enigma of ecological communities.

Author contributions: A.M.d.R. designed research, performed research, analyzed data, and wrote the paper.

The author declares no competing interest.

This article is a PNAS Direct Submission.

[1]Email: A.M.deRoos@uva.nl.

This article contains supporting information online at https://www.pnas.org/lookup/suppl/doi:10.1073/pnas.2023709118/-/DCSupplemental.

Published May 21, 2021.

and their strength have been the conceptual foundation of virtually all existing studies on ecological community stability (24). Even studies assessing stability of real-life communities (25) aim at estimating how species in a community affect each other's population-level growth rate to construct the community matrix (5). But within populations individuals by definition differ and not only because juveniles grow and mature while adults reproduce. Juveniles and adults also differ in their body size and therefore in their ecology (26, 27). Because juveniles are smaller, they generally feed at lower rates (28), are more food limited (29), and are more vulnerable to predation (30, 31). These body size-dependent differences translate into an asymmetry in foraging and predation risk between juveniles and adults, which has been shown to affect structure and dynamics of ecological communities (32).

To study the impact of these asymmetries in foraging and predation risk between juvenile and adult individuals on community diversity and stability I simulated dynamics of randomly constructed, stage-structured model food webs, in which juveniles were more food limited and more exposed to predation than adults, and compared them with dynamics of an analogous model without stage structure (*Materials and Methods*). Species in the food web differed in body weight with only the smallest—basal—species following self-regulating population dynamics. Foraging interactions between all nonbasal species were modeled based on their difference in body weight (*Materials and Methods*). To focus exclusively on differences between juveniles and adults in foraging rate and predation mortality and to allow comparison between models with and without population structure, I assumed juveniles and adults to forage at different rates on the same range of prey species with the same preferences and thus have overlapping diets. Juveniles and adults are furthermore preyed upon by the same predator species but at different rates. Asymmetry in resource foraging is represented phenomenologically by a foraging asymmetry factor q, ranging between 0 and 2, with juvenile and adult resource ingestion rate taken proportional to q and $(2-q)$, respectively (Fig. 1). Asymmetry in vulnerability to predation is represented analogously by a predation asymmetry factor ϕ, also ranging between 0 and 2, with predation mortality of juveniles and adults taken proportional to ϕ and $(2-\phi)$, respectively (Fig. 1). For $q=1$ juveniles and adults hence forage at the same rate, such that maturation and reproduction are limited by food to the same extent. If in addition $\phi=1$, juveniles and adults do not differ in their rates of predation mortality either. Juvenile and adult dynamics were modeled using a juvenile–adult structured model (33) in terms of numerical abundances that explicitly accounts for maintenance requirements, which cause maturation and reproduction to halt at low food availabilities. For $q=1$ and $\phi=1$ this stage-structured food web model can be shown to be identical to a food web model without stage structure (*SI Appendix, Model simplification in case of ontogenetic symmetry*). Community dynamics were simulated until density fluctuations of the persisting species had stabilized (*Materials and Methods*).

Generally, juvenile individuals are far more vulnerable to predation than adults (30, 31). Empirical observations on predator–prey body size ratios have revealed that this ratio is roughly an order of magnitude smaller when it is computed on the basis of the average body size in the predator and prey population than when it is computed as the average body-size ratio between individual predators and the individual prey in their gut (34, 35). This order of magnitude difference suggests that small individuals in a prey population are up to 10 times more likely to be preyed upon than large individuals. Furthermore, per-capita reproduction rates are for most species less limited by food than juvenile maturation rates, in particular because offspring sizes are small compared to adult body sizes (32). A competitive asymmetry between juveniles and adults is further supported by the occurrence of stunted populations in fish (36, 37), shellfish (38), and dragonflies (39) and the asymmetry observed in intraspecific competition experiments (29, 40, 41). Therefore, $q=0.7$ and $\phi=1.8$ are adopted as default values for the juvenile–adult ingestion and predation asymmetry parameter (but see *SI Appendix*, Fig. S1 for the effect of varying q and ϕ).

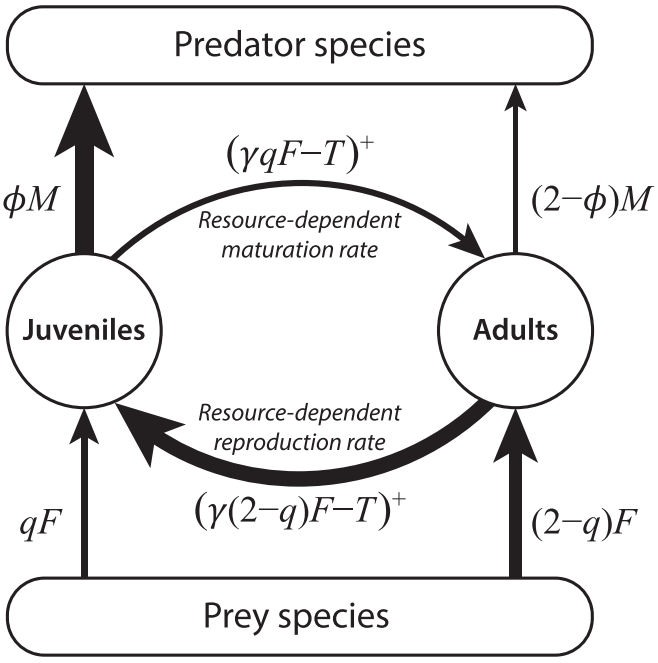

Fig. 1. Basic juvenile–adult structured food web module. Juveniles and adults are assumed to forage with identical preferences on the same prey species at per-capita rate qF and $(2-q)F$, respectively, where q represents the juvenile–adult ingestion asymmetry and F the functional response of the species. Juveniles and adults are preyed upon by the same predator species, dying from predation at per-capita rates ϕM and $(2-\phi)M$, respectively, where ϕ represents the juvenile–adult asymmetry in vulnerability to predation and M represents the species-specific predation pressure. Per-capita maturation and reproduction rates equal $(\gamma qF-T)^+$ and $(\gamma(2-q)F-T)^+$, respectively, where the superscript $+$ indicates restriction of these rates to nonnegative values. Maturation and reproduction stop when food availability F drops below $T/(\gamma q)$ and $T/(\gamma(2-q))$, respectively, and all ingestion is used to cover maintenance requirements. Default parameter values are $q=0.7$ and $\phi=1.8$, reflecting that maturation is more resource limited than reproduction and juveniles are more vulnerable to predation than adults (graphically represented by arrows of different thickness). See *Materials and Methods* for more details.

When juveniles are more limited by food and are more predator sensitive than adults ($q=0.7$, $\phi=1.8$), the structured model results in communities with on average 20 or more nonbasal species persisting on the single basal species (Fig. 2). In contrast, food web simulations with the corresponding unstructured model result in persistence of on average 3 to 4 nonbasal species (Fig. 2 and *SI Appendix*, Fig. S1). This increase in community diversity due to juvenile–adult asymmetry is larger at higher system productivity (*SI Appendix*, Fig. S2). In addition to increasing community diversity juvenile–adult asymmetry also increases the complexity of the food web that structures the community. Food webs resulting from model simulations without stage structure are simple, mostly linear food chains, with most species foraging on a single prey and vulnerable to a single predator (Fig. 2 and *SI Appendix*, Fig. S3). In contrast, food webs resulting from simulations with juvenile–adult asymmetry are complex with most species foraging on multiple prey species and exposed to predation by multiple consumer species (Fig. 2 and *SI Appendix*, Fig. S3). Diverse and complex communities occur in particular when predation on juveniles is 8 to 10 times larger than on adults and

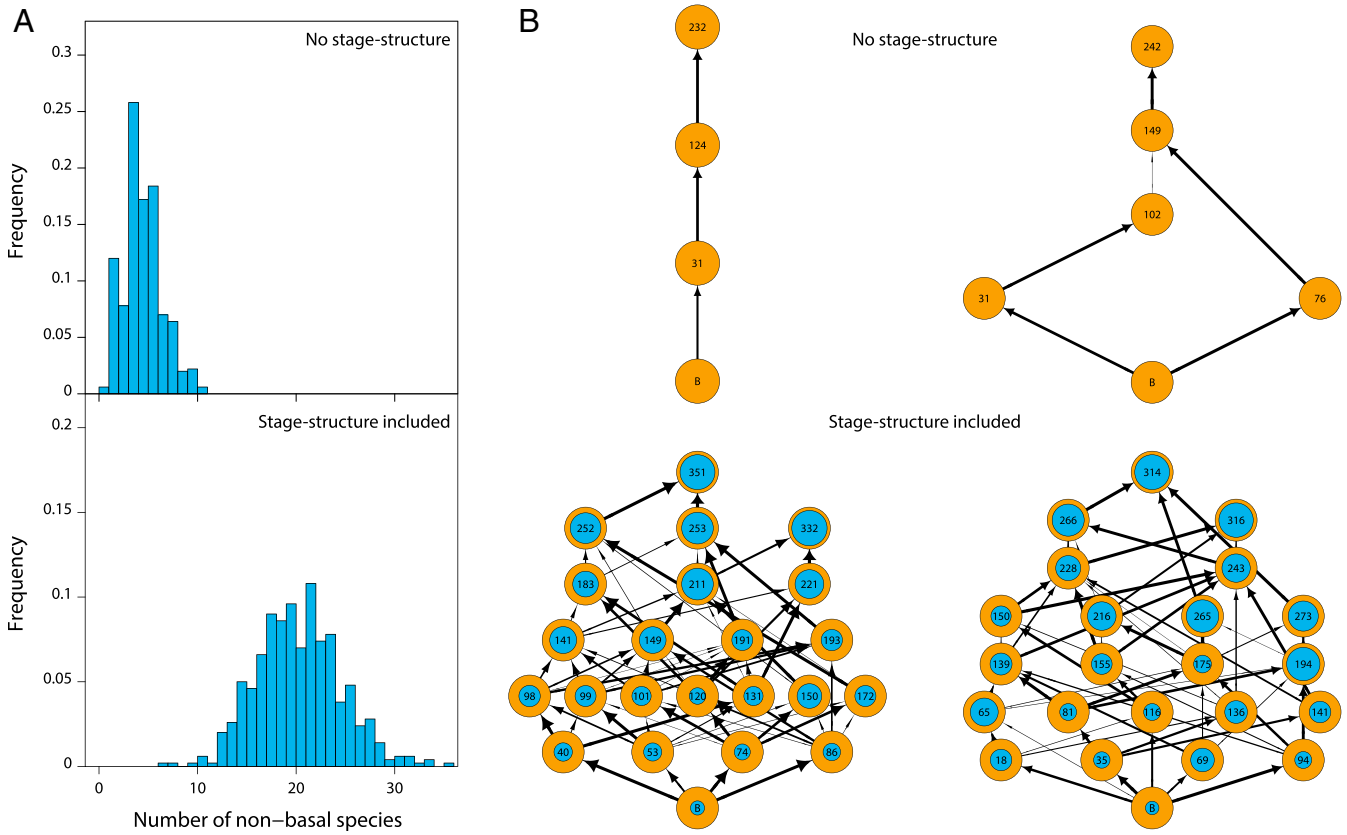

Fig. 2. Juvenile–adult stage structure increases community size and complexity. (*A*) Frequency distribution of community sizes (nonbasal species only) and (*B*) examples of food webs resulting from 500 replicate food web simulations without stage structure (*Top*) and including stage structure with foraging and predation asymmetry between juveniles and adults (*Bottom*). In *B* vertical positions indicate trophic level. Inner circles in *Bottom* row indicate the density of juveniles as fraction of total population density. Arrow widths indicate the relative feeding preference of consumers for a particular prey species.

is less dependent on foraging differences (*SI Appendix*, Figs. S1 and S7).

Temporal dynamics of food webs that result from model simulations without stage structure are characterized by large-amplitude fluctuations in species abundances reminiscent of classical predator–prey cycles (Fig. 3). The cycle amplitudes moreover increase with increasing community size especially because minimum species densities during the cycle decrease (Fig. 3),

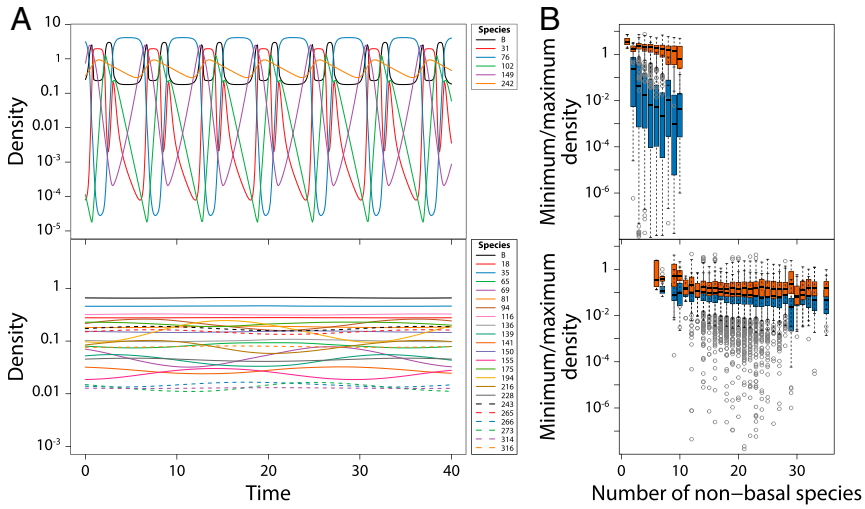

Fig. 3. Juvenile–adult stage structure stabilizes community dynamics. (*A*) Examples of dynamics of all species in food web simulations without stage structure (*Top*) and including stage structure with foraging and predation asymmetry between juveniles and adults (*Bottom*). Corresponding food web structures are shown in Fig. 2 *B*, *Right*. (*B*) Boxplot of minimum (blue bars) and maximum (red bars) total densities of all populations as a function of community size for all persisting species in 500 replicate food web simulations without (*Top*) and with stage structure and foraging and predation asymmetry between juveniles and adults (*Bottom*).

ultimately leading to species extinction and reductions in community diversity. In contrast, the complex food webs resulting from the structured model with juvenile–adult asymmetry either are stable or exhibit small-amplitude fluctuations in total species densities (Fig. 3). Furthermore, if fluctuations in total species densities occur, their amplitude is unaffected by community size (Fig. 3).

When juveniles are more limited by food and more predator sensitive than adults, 22% of the food webs generated by the structured model approach a stable community equilibrium (*Materials and Methods* and *SI Appendix, Computing eigenvalues of the stage-structured model*). These stable communities allow for disentangling how food web interactions and population structure together affect community stability. The structured model in terms of juvenile and adult abundances can be transformed into an equivalent model, in which each species is represented by its total density and the fraction of juveniles in it. The transformation separates the model into a "total species-density subsystem" and a complementary "species-structure subsystem." Community stability is now determined by the stability of each of these two subsystems on their own and their interactions (*Materials and Methods*). The stability of the species-density subsystem on its own is determined by the usual community matrix, measuring the per-capita effect of species on each other's growth rate. For all stable communities resulting from the structured model in the case of juvenile–adult asymmetry the dominant eigenvalue of this community matrix is positive and large (Fig. 4*A*). The community matrix hence predicts these communities to be highly unstable, which mostly results because only the basal species is regulated by a negative self-effect, top predators have no self-effect, and all other nonbasal species exhibit positive self-effects (*Materials and Methods* and *SI Appendix*, Fig. S5). The dominant eigenvalue of the Jacobian matrix determining the stability of the coupled subsystems of species density and species structure, however, has a negative real part for all stable communities (Fig. 4*A*) mostly because the species-density subsystem is connected to and interacts with the species-structure subsystem and the dominant eigenvalue of the matrix determining the stability of this species-structure subsystem on its own has a negative real part. The large differences between the dominant eigenvalues of the community and Jacobian matrices indicate that the dynamic nature of the fraction of juveniles of the species is key to community stability.

Simulations of community dynamics starting from stable community states confirm the stabilizing impact of dynamic population structure and how it increases the resilience of the community: Even after a disturbance that reduces the density of all species by 50% the complete model involving the coupled species-density and species-structure subsystems predicts a rapid return to the stable community equilibrium (Fig. 4*C*). The reduction in density at most results in the extinction of a few species (*SI Appendix*, Fig. S6). In contrast, when starting in the undisturbed community equilibrium and simulating dynamics using only the species-density subsystem with for each species the fraction of juveniles constant and equal to its equilibrium value, species densities soon start to fluctuate wildly (Fig. 4*C*). Consequently, most species eventually go extinct and the community ends up being of similar size to the communities predicted by the food web model without population structure (*SI Appendix*, Fig. S6). Similar results were obtained with an alternative method (42) to represent the stage structure of each species by a single measure of species density. Likewise, starting in the undisturbed community equilibrium and simulating dynamics using a corresponding, age-structured model, in which the juvenile maturation rate is set constant in time and equal to its equilibrium value, wild fluctuations in species density soon develop (Fig. 4*C*) and the community eventually ends up being of similar size to the communities predicted by the food web model without population structure (*SI Appendix*, Fig. S6).

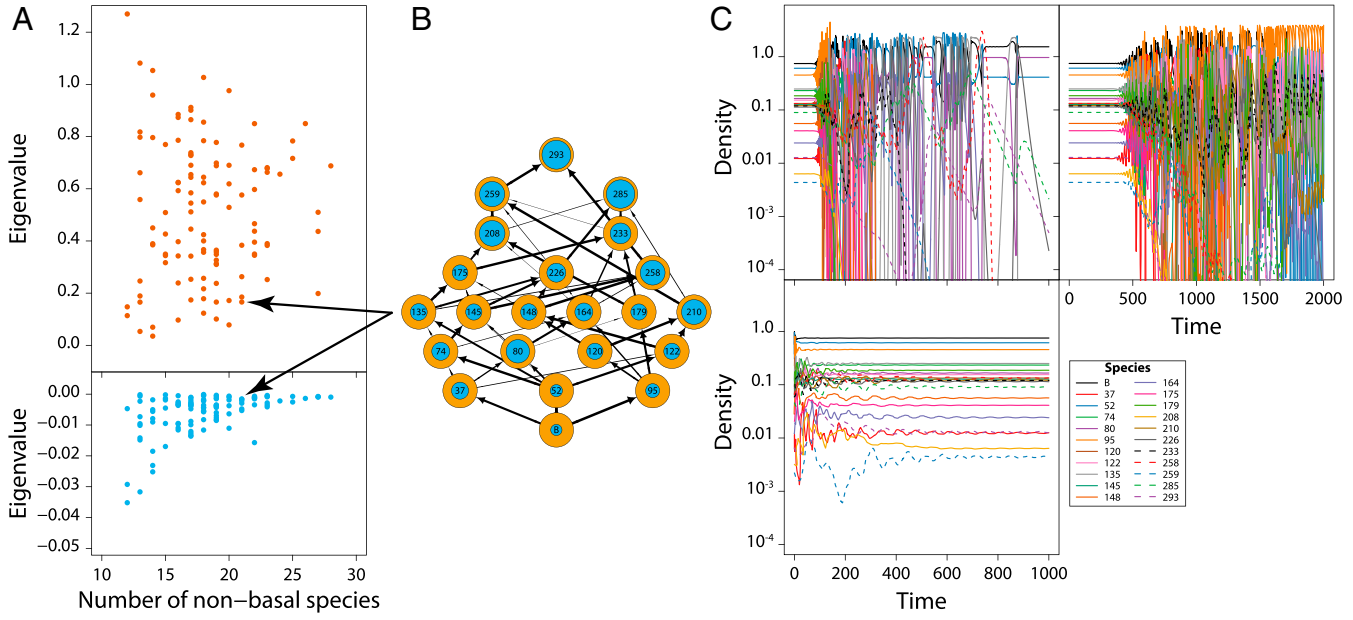

Fig. 4. Adaptive stage structure stabilizes community dynamics. (*A*) Real part of the dominant eigenvalue of the community matrix (*Top*) and the Jacobian matrix determining community stability (*Bottom*) as a function of community size for all stable communities resulting from simulations with the stage-structured model and foraging and predation asymmetry between juveniles and adults (*Materials and Methods*). (*B*) Example of a stable community with 21 nonbasal species. (*C*) Dynamics of the community shown in *B* with a constant juvenile–adult density ratio equal to its equilibrium value for each species and initial densities equal to their equilibrium densities (*Top Left*), with a constant juvenile maturation rate equal to its equilibrium value for each species and initial densities equal to their equilibrium densities (*Top Right*, model equivalent with an analogous age-structured model), and with dynamic juvenile–adult stage structure following a disturbance event that reduces the densities of all species in the community by 50% (*Bottom*) (*Materials and Methods*).

Stability of these model communities therefore depends on the dynamic changes in juvenile–adult ratio in the population and on the food dependence of both the maturation and the reproduction rate. The dynamics of the juvenile fraction in each of the species dampen density fluctuations in the community in various ways. For example, increases in reproduction of one particular species have more limited effects on its prey species and are more quickly quenched by its predators, when juveniles forage at lower rates and are more vulnerable to predation, than in the absence of any population structure. Increases in food availability for a particular focal species will lead to modulation of the interaction strength with its prey, as higher prey densities will speed up maturation, increase the fraction of adults, and thus increase the average per-capita impact of the species on its prey. Furthermore, a dynamic population stage structure also buffers against fluctuations in predation pressure, as increases in predation will primarily affect the juveniles that are limited most by food availability. Higher mortality under these conditions has been shown to relax possible bottlenecks in juvenile maturation and to increase the efficiency with which resources are used for population growth as opposed to being used for somatic maintenance (33, 43). Thus, dynamic population stage structure leads to adaptive modulation of the average interaction strength between species that counters fluctuations in bottom-up and top-down effects.

The presented results are robust to changes in the population stage structure as well as the model describing dynamics of each of the species. Similar results regarding community diversity, complexity, and dynamics are obtained under even wider parameter ranges when populations are represented by the biomass densities in three life history stages (small juveniles, larger immatures, and adults) as opposed to numerical abundances of juveniles and adults only and the dynamics of each population are modeled using a stage-structured biomass model that approximates the dynamics of a complete population body size distribution (*Materials and Methods* and *SI Appendix, Stage-structured biomass model of species dynamics* and Figs. S7–S9). The communities resulting from this more detailed model tend to be even larger with on average 25 to 30 species coexisting on a single basal species.

The topology of the interaction network between species in a community, which forms the theoretical foundation of existing studies on community stability, may hence provide only partial insight into the mechanisms stabilizing complex communities and may even suggest necessary conditions for stability, such as ubiquitous self-regulation, that might prove too restrictive once the dynamics of population stage structure are taken into account. As shown here, the dynamic population structure can simply overrule the destabilizing effects of the species interaction network. This within-species mechanism thus breaks up in a realistic and natural way the constraints on community complexity that were originally identified by May (6, 7) and extends the range of mechanisms and constraints on community interactions that have been identified to promote stability using species-based approaches (13–18). If we are to model the impact of environmental change on complex ecological communities, we need models that can fully capture the diversity, complexity, stability, and vulnerability of these systems—this study represents a major advance on existing approaches that consider only species-level interaction networks.

Materials and Methods

Food Web Construction. Model food webs are constructed by assigning each of an initial $N = 500$ species random niche values n_i between 0 and 1. Niche values are related to body size w_i following $w_i = (w_{max})^{n_i}(w_{min})^{(1-n_i)}$ with minimum and maximum species body size equal to $w_{min} = 10^{-8}$ and $w_{max} = 10^4$ g, respectively (*SI Appendix*, Fig. S10). To represent documented prey–predator body size ratios (35, 44) more faithfully than in the niche model (45) the center c_i of the feeding niche of consumer species i is uniformly distributed between $n_i - 2.5/^{10}\log(w_{max}/w_{min})$ and $n_i - 0.5/^{10}\log(w_{max}/w_{min})$, resulting in median prey–predator body size ratios between $10^{-2.5}$ and $10^{-0.5}$. The width r_i of the feeding niche equals $1/^{10}\log(w_{max}/w_{min})$, such that consumer species i feeds on prey species with body sizes ranging between $(w_{max})^{(c_i-r_i/2)}(w_{min})^{(1-(c_i-r_i/2))}$ and $(w_{max})^{(c_i+r_i/2)}(w_{min})^{(1-(c_i+r_i/2))}$. The relative preference ψ_{ik} of consumer i for prey k follows a piecewise continuous hump-shaped distribution with finite range (Bates distribution of order 3):

$$\psi_{ik} = \begin{cases} 6\left(\frac{n_k - c_i}{r_i} + \frac{1}{2}\right)^2 & \text{if } -\frac{1}{2} \le \frac{n_k - c_i}{r_i} < -\frac{1}{6} \\ -12\left(\frac{n_k - c_i}{r_i} + \frac{1}{2}\right)^2 + 12\left(\frac{n_k - c_i}{r_i} + \frac{1}{2}\right) - 2 & \text{if } -\frac{1}{6} \le \frac{n_k - c_i}{r_i} < \frac{1}{6} \\ 6\left(\frac{n_k - c_i}{r_i} - \frac{1}{2}\right)^2 & \text{if } \frac{1}{6} \le \frac{n_k - c_i}{r_i} < \frac{1}{2} \\ 0 & \text{otherwise.} \end{cases} \quad [1]$$

Food Web Dynamics without Stage Structure. Species are ranked according to their niche value (i.e., body size) and their numerical abundances are indicated with C_i. The basal species (with index 1) is assumed to forage on its own exclusive resource R, the dynamics of which are described by

$$\frac{dR}{dt} = P - \delta R - \alpha_1 R C_1 \quad [2]$$

with P the productivity of the resource and δ its turnover rate, while α_1 scales the predation pressure of the basal species on its resource. The resource dynamics are assumed to be in pseudo-steady state, such that $R = P/(\delta + \alpha_1 C_1)$ at all times. The (linear) functional response of the basal species, indicated with F_1, is consequently assumed to equal the pseudo-steady-state value of R:

$$F_1 = \frac{P}{\delta + \alpha_1 C_1}. \quad [3]$$

Nonbasal species are assumed to forage following a type II functional response on all other species in the community at a relative rate ψ_{ik} (Eq. **1**) determined by the species body size ratio. The encounter rate of a consumer species with index i with all its prey species (indexed with k) therefore equals

$$E_i = \sum_{k<i} \psi_{ik} C_k \quad [4]$$

and its functional response F_i (scaled between 0 and 1) equals

$$F_i = \frac{E_i}{H_i + E_i} \quad [5]$$

with H_i the consumer's half-saturation density. Because the prey–predator body size ratio is assumed to be strictly smaller than 1, consumer species i can only forage on all species with index $k < i$.

The dynamics of all species densities are now described by

$$\frac{dC_i}{dt} = \gamma_i F_i C_i - (T_i + \mu_i) C_i - C_i \sum_{k>i} \alpha_k \psi_{ki} \frac{C_k}{H_k + E_k}, \quad [6]$$

where E_i and F_i represent the value of the food encounter rate and the scaled functional response of species i, respectively. The parameter γ_i relates the growth rate of species i to its functional response F_i, while α_i scales the predation pressure of species i on its prey species. The parameters T_i and μ_i represent the population loss rate through somatic maintenance costs and background mortality, respectively. Note that all species are ordered according to their body size and hence only species with an index $k > i$ can feed on species i.

Food Web Dynamics with Stage Structure. Numerical abundances of juvenile and adult individuals of consumer species i are indicated with J_i and A_i, respectively. Juveniles and adults are assumed to feed on the same range of prey species, have the same prey preferences, and thus have overlapping diets. However, juveniles and adults feed at different rates, such that the foraging rates of juveniles and adults of species i equal $q\alpha_i F_i$ and $(2 - q)\alpha_i F_i$, respectively, with proportionality constants α_i and F_i the functional response of species i.

ECOLOGY

Juveniles and adults are also assumed to differ in their sensitivity to predation, such that the predation mortality experienced by juveniles and adults of species i equals ϕM_i and $(2-\phi)M_i$, respectively, where M_i represents the predation pressure exerted on species i by all of its predators. The parameters q and ϕ are referred to as the foraging and predation asymmetry between juveniles and adults.

The functional response for the basal species is defined analogously to the model without stage structure, taking into account the foraging asymmetry between juveniles and adults,

$$F_1 = \frac{P}{\delta + \alpha_1 \left(qJ_1 + (2-q)A_1\right)}, \quad [7]$$

while the encounter rate with prey for nonbasal species equals

$$E_i = \sum_{k<i} \psi_{ik} \left(\phi J_k + (2-\phi)A_k\right). \quad [8]$$

The expression for the functional response of nonbasal species remains the same (Eq. **5**). In addition to decreasing through background mortality the numerical abundances of juvenile and adult individuals change through reproduction and maturation. These processes are described by a stage-structured model (33) that assumes maturation and reproduction to stop when food availability drops below a threshold level and food intake is not sufficient to cover basic maintenance costs. In particular, maturation of juveniles of species i depends on its functional response F_i, following

$$m_i(F_i) = \max(\gamma_i q F_i - T_i, 0), \quad [9]$$

while reproduction by adults follows

$$b_i(F_i) = \max(\gamma_i (2-q) F_i - T_i, 0). \quad [10]$$

Analogous to the model without stage structure the parameter γ_i relates maturation and reproduction to the food availability, qF_i and $(2-q)F_i$, for juveniles and adults, respectively. The maximum functions in the expressions for $m_i(F_i)$ and $b_i(F_i)$ ensure that maturation and reproduction halt whenever food availability F_i drops below $T_i/(q\gamma_i)$ and $T_i/((2-q)\gamma_i)$, respectively. The parameter q hence determines in a phenomenological manner whether maturation ($q<1$) or reproduction ($q>1$) is more limited by food availability.

Dynamics of the juvenile–adult structured food web model are described by

$$\frac{dJ_i}{dt} = b_i(F_i)A_i - m_i(F_i)J_i - \mu_i J_i - \phi J_i M_i \quad [11]$$

$$\frac{dA_i}{dt} = m_i(F_i)J_i - \mu_i A_i - (2-\phi)A_i M_i \quad [12]$$

with

$$M_i = \sum_{k>i} \alpha_k \psi_{ki} \frac{qJ_k + (2-q)A_k}{H_k + E_k} \quad [13]$$

the predation pressure exerted on species i by all of its predators.

Model Parameterization. Parameter values were randomly selected, but constrained by default scaling relationships with species body size as presented by de Roos and Persson (ref. 32, boxes 3.3 and 3.4), except that the time variable and hence all rate parameters have been scaled by a factor of 10 to speed up numerical computations. The default parameter scaling relationships with body size reflect documented generalities (28, 46, 47) that maximum ingestion rates are roughly an order of magnitude larger than maintenance rates, that conversion efficiency is roughly 60%, and that losses through background mortality are 7 to 10 times smaller than losses through maintenance. More specifically, for each nonbasal species, the half-saturation density H_i occurring in its functional response F_i was sampled uniformly from the interval [0.5,2.5]. The parameters α_i, γ_i, T_i, and μ_i were assumed to scale with $w_i^{-0.25}$. For each species i the values of these parameters were generated using the equations

$$\alpha_i = \alpha_0 \left(1 + 2\sigma_\alpha (x_{i1} - 1/2)\right) w_i^{-0.25}$$
$$\gamma_i = \gamma_0 \left(1 + 2\sigma_\gamma (x_{i2} - 1/2)\right) w_i^{-0.25}$$
$$T_i = T_0 \left(1 + 2\sigma_T (x_{i3} - 1/2)\right) w_i^{-0.25}$$
$$\mu_i = \mu_0 \left(1 + 2\sigma_\mu (x_{i4} - 1/2)\right) w_i^{-0.25}$$

with $\alpha_0 = 1.0$, $\gamma_0 = 0.6$, $T_0 = 0.1$, and $\mu_0 = 0.015$ the default mean values of the species-specific parameters (32). The species-specific parameters α_i, γ_i, T_i, and μ_i were for each species randomly selected from a Bates distribution of degree 3 around these mean values. The Bates distribution is the continuous probability distribution of the mean, X, of three independent uniformly distributed random variables on the unit interval. Random values from this distribution range between 0 and 1 with mean value of $1/2$. The quantities x_{ij} are independent realizations of the random variable X, while σ_α, σ_γ, σ_T, and σ_μ represent the one-sided, relative width of the distributions of the species-specific parameters α_i, γ_i, T_i, and μ_i, respectively, around their mean values. Default values for these relative widths equal 0.1, such that all species-specific parameters range between 0.9 and 1.1 times their default, mean value and follow hump-shaped distributions within these ranges. Finally, the productivity P and turnover rate δ of the exclusive resource for the basal species were taken equal to 60 and 2.0, respectively, in all computations, unless stated otherwise. The two remaining parameters in the model, the foraging asymmetry parameter q and the predation asymmetry parameter ϕ, were varied between the different computations to assess their effect on community dynamics.

Numerical Simulation Procedure. Numerical integrations of the food web with $N = 500$ species were carried out using an adaptive Runge–Kutta method implemented in C. Relative and absolute tolerances during the integration were set to 10^{-7} and 10^{-13}, respectively. During the first 10^4 time units no species were removed from the community, even if they attained very low density. For $t > 10^4$ each species, whose total density $J_i + A_i$ dropped below 10^{-8}, was removed from the community. This persistence threshold ensures that the product of the relative tolerance (10^{-7}) and the lowest species density (10^{-8}) is larger than the machine precision (equal to $1.11 \cdot 10^{-16}$ according to the Institute of Electrical and Electronics Engineers (IEEE) 754-2008 standard in the case of double precision). During numerical computations mean and variance as well as the maximum and minimum values of the total species density $J_i + A_i$ were continuously monitored for all species. The values of these measured statistics are reset whenever the community structure changes as one or more species in the community go extinct. Numerical integrations are halted whenever the community structure has not changed for 10^6 time units and no change has occurred from one time unit to the next in the values of these statistics (mean, minimum, maximum, and variance of total species density) for all species in the community.

Sources of Community Stability. Through analytical manipulations the model in terms of juvenile abundances J_i and adult abundances A_i can be recast into an equivalent model in terms of total species abundance $C_i = J_i + A_i$ and the fraction of juveniles in a population $Z_i = J_i/C_i$. In terms of these alternative model variables the functional response value for the basal species can be written as

$$F_1 = \frac{P}{\delta + \alpha_1 \left(qZ_1 + (2-q)(1-Z_1)\right) C_1} \quad [14]$$

while the encounter rate with prey for nonbasal species equals

$$E_i = \sum_{k<i} \psi_{ik} \left(\phi Z_k + (2-\phi)(1-Z_k)\right) C_k. \quad [15]$$

The dynamics of total species density and fraction of juveniles in all populations are then described by

$$\frac{dC_i}{dt} = b_i(F_i)(1-Z_i)C_i - \mu_i C_i - \left(\phi Z_i + (2-\phi)(1-Z_i)\right) C_i M_i \quad [16]$$

$$\frac{dZ_i}{dt} = b_i(F_i)(1-Z_i)^2 - m_i(F_i)Z_i - 2(\phi - 1)(1-Z_i)Z_i M_i \quad [17]$$

with

$$M_i = \sum_{k>i} \alpha_k \psi_{ki} \frac{\left(qZ_k + (2-q)(1-Z_k)\right) C_k}{H_k + E_k} \quad [18]$$

the predation pressure exerted on species i by all of its predators.

The resulting system of differential equations can hence be written as

$$\frac{d\mathbf{C}}{dt} = \mathbf{K}(\mathbf{C}, \mathbf{Z}) \quad [19]$$

$$\frac{d\mathbf{Z}}{dt} = \mathbf{L}(\mathbf{C}, \mathbf{Z}) \quad [20]$$

in which $\mathbf{C}$ and $\mathbf{Z}$ indicate vectors of all total species abundances and fractions of juveniles in all populations, respectively. The vector-valued functions

K(**C**, **Z**) and **L**(**C**, **Z**) contain the right-hand side of the differential equations dC_i/dt for the species-density subsystem and dZ_i/dt for the species-structure subsystem, respectively. For a system with m species the Jacobian matrix J of the ordinary differential equations above is a $2m \times 2m$ matrix of the form

$$J = \begin{pmatrix} \frac{\partial \mathbf{K}}{\partial \mathbf{C}} & \frac{\partial \mathbf{K}}{\partial \mathbf{Z}} \\ \frac{\partial \mathbf{L}}{\partial \mathbf{C}} & \frac{\partial \mathbf{L}}{\partial \mathbf{Z}} \end{pmatrix}. \quad [21]$$

Each of the four parts of J is a $m \times m$ matrix containing the partial derivatives of the functions **K**(**C**, **Z**) and **L**(**C**, **Z**) with respect to the total species densities ($C_1, \ldots, C_m$) and fractions of juveniles ($Z_1, \ldots, Z_m$). Expressions for these partial derivatives are provided in *SI Appendix, Computing eigenvalues of the stage-structured model*.

All communities resulting from the stage-structured model with asymmetry in feeding and predation between juveniles and adults ($q = 0.7$, $\phi = 1.8$) for which the minimum and maximum values of the total species density differ less than 10^{-6} for all species are classified as stable. Communities for which minimum and maximum values of total density of at least one species differed more than 10^{-6} from each other are considered unstable (cycling). For both stable and unstable communities the average total abundance and fraction of juveniles observed in the simulation were used as starting values to numerically solve for the equilibrium state using the package "rootSolve" (48, 49) in R (50). For all 115 stable communities the equilibrium community state was successfully located and was numerically indistinguishable from the average densities and juvenile fractions observed in the numerical simulations. For 147 communities that were considered unstable (cycling) the numerical solution procedure also converged to an equilibrium community state with all species present, while for 238 unstable communities the numerical solution procedure did not converge to such an equilibrium state. For all equilibrium community states found, the Jacobian matrix J is evaluated by substituting for all species the equilibrium value for total abundance and fraction of juveniles as well as all general and species-specific parameters into the expressions for the elements of J. The eigenvalues of the Jacobian matrix are subsequently computed using the routine eigen() in R (Fig. 4 *A*, *Bottom*, for stable communities only; see *SI Appendix*, Fig. S4 for both stable and unstable communities).

To evaluate how dynamic changes in population stage structure (i.e., changes in the juvenile–adult ratio) affect community stability, the eigenvalues of the Jacobian matrix J of stable communities are compared with the eigenvalues of the top-left submatrix of J, the $m \times m$ matrix $\partial \mathbf{K}/\partial \mathbf{C}$. The latter matrix determines the stability of the species-density subsystem on its own with the juvenile fraction of each species equal to its equilibrium value. This matrix also corresponds to the community matrix with elements $\partial(dC_i/dt)/\partial C_j$ capturing the per-capita effect of the species in the community on each other's growth rate. The community matrix determines the stability of a model, in which the dynamics of total species densities follow the same set of equations as in the full model, but the fraction of juveniles in the populations is constant over time and equals the fraction of juveniles of the species at equilibrium (Fig. 4 *A*, *Top*). Comparing the eigenvalues of the Jacobian matrix J and the community matrix reveals the impact of dynamic changes in the population structure of the species on the stability of the community equilibrium (*SI Appendix, Computing eigenvalues of the stage-structured model*).

To further assess the differences between constant and dynamic juvenile fractions in the populations, for all stable communities resulting from the stage-structured model with asymmetry in feeding and predation between juveniles and adults ($q = 0.7$, $\phi = 1.8$) community dynamics were computed starting from the equilibrium community state using the reduced model including the differential equations dC_i/dt for the species-density subsystem only, with the juvenile fraction Z_i in each of the populations taken equal to its equilibrium value inferred from the stable community state (Fig. 4 *C*, *Top Left* and *SI Appendix, Sources of community stability* and Fig. S6). Similarly, community dynamics were computed with an age-structured analogue of the full model including differential equations dC_i/dt for the species-density subsystem and dZ_i/dt for the species-structure subsystem, but with the juvenile maturation rate $m_i(F_i)$ for each of the species in the community taken constant in time and equal to the maturation rate in the equilibrium community state. These simulations were also started from the equilibrium community state (Fig. 4 *C*, *Top Right* and *SI Appendix, Sources of community stability* and Fig. S6). Finally, community dynamics were computed with the full model including the differential equations dC_i/dt for the species-density subsystem and dZ_i/dt for the species-structure subsystem and dynamic changes in the juvenile maturation rates starting from a community state in which the initial density of each species was exactly 50% of its equilibrium value as inferred from the stable community state (Fig. 4 *C*, *Bottom* and *SI Appendix*, Fig. S6).

Extent of Self-Regulation. For stable communities the extent of self-regulation of species is assessed with the diagonal elements of the community matrix, the $m \times m$ matrix $\partial \mathbf{K}/\partial \mathbf{C}$, which measures the positive or negative effect of the total species abundance C_i on its own rate of change dC_i/dt (*SI Appendix*, Fig. S5).

Data Availability. All code, data files, and R scripts used to generate the figures are available in Bitbucket at https://bitbucket.org/amderoos/structuredfoodweb/.

ACKNOWLEDGMENTS. I thank Bernd Blasius, Jennifer Dunne, Jacopo Grilli, Bob Holt, Kevin Lafferty, Ben Martin, Lennart Persson, Axel Rossberg, and Peter de Ruiter for stimulating discussions and their comments on the manuscript and the Santa Fe Institute for the hospitality while carrying out this research.

1. T. W. Schoener, "Resource partitioning" in *Community Ecology Pattern and Process*, J. Kilkkawa, D. J. Anderson, Eds. (Blackwell Scientific, Boston, MA, 1986), pp. 91–126.
2. J. A. Wiens, Spatial scaling in ecology. *Funct. Ecol.* **3**, 385–397 (1989).
3. X. Chen, J. E. Cohen, Transient dynamics and food-web complexity in the Lotka-Volterra cascade model. *Proc. Biol. Sci.* **268**, 869–877 (2001).
4. R. J. Williams, N. D. Martinez, Stabilization of chaotic and non-permanent food-web dynamics. *Euro. Phys. J. B* **38**, 297–303 (2004).
5. R. Levins, *Evolution in Changing Environments: Some Theoretical Explorations* (Princeton University Press, Princeton, NJ, 1968).
6. R. M. May, Will a large complex system be stable? *Nature* **237**, 413–414 (1972).
7. R. M. May, *Stability and Complexity in Model Ecosystems* (Princeton University Press, Princeton, NJ, 1973).
8. R. MacArthur, Fluctuations of animal populations and a measure of community stability. *Ecology* **36**, 533–536 (1955).
9. R. T. Paine, Food web complexity and species diversity. *Am. Nat.* **100**, 65–75 (1966).
10. K. S. McCann, The diversity-stability debate. *Nature* **405**, 228–233 (2000).
11. T. Namba, Multi-faceted approaches toward unravelling complex ecological networks. *Popul. Ecol.* **57**, 3–19 (2015).
12. S. Allesina, S. Tang, The stability–complexity relationship at age 40: A random matrix perspective. *Popul. Ecol.* **57**, 63–75 (2015).
13. A. M. Neutel, J. A. P. Heesterbeek, P. C. De Ruiter, Stability in real food webs: Weak links in long loops. *Science* **296**, 1120–1123 (2002).
14. M. Kondoh, Foraging adaptation and the relationship between food-web complexity and stability. *Science* **299**, 1388–1391 (2003).
15. U. Brose, R. J. Williams, N. D. Martinez, Allometric scaling enhances stability in complex food webs. *Ecol. Lett.* **9**, 1228–1236 (2006).
16. S. L. Pimm, J. H. Lawton, On feeding on more than one trophic level. *Nature* **275**, 542–544 (1978).
17. E. Thébault, C. Fontaine, Stability of ecological communities and the architecture of mutualistic and trophic networks. *Science* **329**, 853–856 (2010).
18. J. Grilli, G. Barabás, M. J. Michalska-Smith, S. Allesina, Higher-order interactions stabilize dynamics in competitive network models. *Nature* **548**, 210–213 (2017).
19. G. Barabás, M. J. Michalska-Smith, S. Allesina, Self-regulation and the stability of large ecological networks. *Nat. Ecol. Evol.* **1**, 1870–1875 (2017).
20. P. Yodzis, The stability of real ecosystems. *Nature* **289**, 674–676 (1981).
21. R. W. Sterner, A. Bajpai, T. Adams, The enigma of food chain length: Absence of theoretical evidence for dynamic constraints. *Ecology* **78**, 2258–2262 (1997).
22. S. L. Pimm, *Food Webs* (University of Chicago Press, Chicago, IL, 2002).
23. J. M. Chase *et al.*, The interaction between predation and competition: A review and synthesis. *Ecol. Lett.* **5**, 302–315 (2002).
24. M. Pascual, J. A. Dunne, "From small to large ecological networks in a dynamic world" in *Ecological Networks Linking Structure to Dynamics in Food Webs*, M. Pascual, J. A. Dunne, Eds. (Oxford University Press, New York, NY, 2006), pp. 3–24.
25. C. Jacquet *et al.*, No complexity-stability relationship in empirical ecosystems. *Nat. Commun.* **7**, 12573–12578 (2016).
26. E. E. Werner, J. F. Gilliam, The ontogenetic niche and species interactions in size structured populations. *Annu. Rev. Ecol. Syst.* **15**, 393–425 (1984).
27. T. E. X. Miller, V. H. W. Rudolf, Thinking inside the box: Community-level consequences of stage-structured populations. *Trends Ecol. Evol.* **26**, 457–466 (2011).
28. R. H. Peters, *The Ecological Implications of Body Size* (Cambridge Studies in Ecology, Cambridge University Press, Cambridge, UK, 1983).
29. T. Potter, L. King, J. Travis, R. D. Bassar, Competitive asymmetry and local adaptation in Trinidadian guppies. *J. Anim. Ecol.* **88**, 330–342 (2018).
30. S. M. Sogard, Size-selective mortality in the juvenile stage of teleost fishes: A review. *Bull. Mar. Sci.* **60**, 1129–1157 (1997).
31. G. Woodward, D. C. Speirs, A. G. Hildrew, Quantification and resolution of a complex, size-structured food web. *Adv. Ecol. Res.* **36**, 85–135 (2005).

32. A. M. de Roos, L. Persson, *Population and Community Ecology of Ontogenetic Development* (Monographs in Population Biology, Princeton University Press, Princeton, NJ, 2013), vol. 51.
33. A. M. de Roos, When individual life history matters: Conditions for juvenile-adult stage structure effects on population dynamics. *Theor. Ecol.* **11**, 397–416 (2018).
34. G. Woodward, P. H. Warren, "Body size and predatory interactions in freshwaters: Scaling from individuals to communities" in *Body Size: The Structure and Function Of Aquatic Ecosystems*, A. G. Hildrew, D. G. Raffaelli, R. Edmonds-Brown, Eds. (Cambridge University Press, Cambridge, UK, 2007), pp. 98–117.
35. T. Nakazawa, M. Ushio, M. Kondoh, Scale dependence of predator–prey mass ratio: Determinants and applications. *Adv. Ecol. Res.* **45**, 269–302 (2011).
36. D. A. Roff, *The Evolution of Life Histories* (Chapman & Hall, New York, NY, 1992).
37. C. J. Chizinski, K. L. Pope, G. R. Wilde, R. E. Strauss, Implications of stunting on morphology of freshwater fishes. *J. Fish. Biol.* **76**, 564–579 (2010).
38. T. M. Saunders, S. Mayfield, A. A. Hogg, A simple, cost-effective, morphometric marker for characterizing abalone populations at multiple spatial scales. *Mar. Freshw. Res.* **59**, 32–40 (2008).
39. J. Van Buskirk, Population consequences of larval crowding in the dragonfly *Aeshna Juncea*. *Ecology* **74**, 1950–1958 (1993).
40. C. A. Narvaez, B. Sainte-Marie, L. E. Johnson, Intraspecific competition in size-structured populations: Ontogenetic shift in the importance of interference competition in a key marine herbivore. *Mar. Ecol. Prog. Ser.* **649**, 97–110 (2020).
41. W. A. Nelson, B. Joncour, D. Pak, O. N. Bjørnstad, Asymmetric interactions and their consequences for vital rates and dynamics: The smaller tea tortrix as a model system. *Ecology* **100**, e02558–15 (2019).
42. A. G. Rossberg, K. D. Farnsworth, Simplification of structured population dynamics in complex ecological communities. *Theor. Ecol.* **4**, 449–465 (2010).
43. A. M. de Roos *et al.*, Food-dependent growth leads to overcompensation in stage-specific biomass when mortality increases: The influence of maturation versus reproduction regulation. *Am. Nat.* **170**, E59–E76 (2007).
44. U. Brose *et al.*, Body sizes of consumers and their resources. *Ecology* **86**, 2545 (2005).
45. R. J. Williams, N. D. Martinez, Simple rules yield complex food webs. *Nature* **404**, 180–183 (2000).
46. P. Yodzis, S. Innes, Body size and consumer resource dynamics. *Am. Nat.* **139**, 1151–1175 (1992).
47. M. W. McCoy, J. F. Gillooly, Predicting natural mortality rates of plants and animals. *Ecol. Lett.* **11**, 710–716 (2008).
48. K. Soetaert, *RootSolve: Nonlinear Root Finding, Equilibrium and Steady-State Analysis of Ordinary Differential Equations* (R package 1.6, 2009).
49. K. Soetaert, P. M. Herman, *A Practical Guide to Ecological Modelling. Using R as a Simulation Platform* (Springer, Dordrecht, The Netherlands, 2009).
50. R Core Team, *R: A Language and Environment for Statistical Computing* (R Foundation for Statistical Computing, Vienna, Austria, 2020).

PNAS
www.pnas.org

Supplementary Information for

Dynamic population stage-structure due to juvenile-adult asymmetry stabilises complex ecological communities

André M. de Roos

Corresponding Author: André M. de Roos.
E-mail: A.M.deRoos@uva.nl

This PDF file includes:

Supplementary text
Figs. S1 to S10 (not allowed for Brief Reports)
SI References

Supporting Information Text

Model reformulation and analysis

The stage-structured model in terms of the juvenile and adult densities J_i and A_i, respectively, can be reformulated into a model in terms of the total number of individuals of species i and the fraction of juveniles in the population of species i. Define C_i as the total density, $C_i = J_i + A_i$, and Z_i as the fraction of juveniles of species i, $Z_i = J_i/C_i$. Using these alternative model variables the functional response value for the basal species can be written as:

$$F_1 = \frac{P}{\delta + \alpha_1 \left(qZ_1 + (2-q)(1-Z_1)\right) C_1} \quad [1]$$

and the encounter rate of all non-basal species with their prey as

$$E_i = \sum_{k<i} \psi_{ik} \left(\phi Z_k + (2-\phi)(1-Z_k)\right) C_k \quad [2]$$

From the ordinary differential equations (ODEs) for the juvenile and adult densities J_i and A_i presented in the Materials and Methods section, the following system of ODEs for the alternative model variables C_i and Z_i can then be derived through analytical manipulation:

$$\frac{dC_i}{dt} = b_i(F_i)(1-Z_i)C_i - \mu_i C_i - \left(\phi Z_i + (2-\phi)(1-Z_i)\right) C_i \sum_{k>i} \alpha_k \psi_{ki} \frac{\left(qZ_k + (2-q)(1-Z_k)\right) C_k}{H_k + E_k} \quad [3]$$

$$\frac{dZ_i}{dt} = b_i(F_i)(1-Z_i)^2 - m_i(F_i)Z_i - 2(\phi-1)(1-Z_i)Z_i \sum_{k>i} \alpha_k \psi_{ki} \frac{\left(qZ_k + (2-q)(1-Z_k)\right) C_k}{H_k + E_k} \quad [4]$$

Model simplification in case of ontogenetic symmetry. Assuming ontogenetic symmetry in ingestion and per-capita predation risk between juveniles and adults is equivalent to setting both q and ϕ equal to 1, which simplifies the per-capita reproduction and maturation rate to:

$$b_i(F_i) = m_i(F_i) = \max\left(\gamma_i F_i - T_i, 0\right)$$

while the expressions for the encounter rate of non-basal species with their prey, E_i, equals:

$$E_i = \sum_{k<i} \psi_{ik} C_k \quad [5]$$

The functional response for species i is hence given by:

$$F_i = \begin{cases} \dfrac{P}{\delta + \alpha_1 C_1} & i = 1 \\ \dfrac{\sum_{k<i} \psi_{ik} C_k}{H_i + \sum_{k<i} \psi_{ik} C_k} & \text{otherwise} \end{cases} \quad [6]$$

The equations describing the dynamics of total species densities C_i and fractions of juveniles Z_i therefore simplify to:

$$\frac{dC_i}{dt} = \max\left(\gamma_i F_i - T_i, 0\right)(1-Z_i)C_i - \mu_i C_i - \sum_{k>i} \alpha_k \psi_{ki} \frac{C_k}{H_k + E_k} C_i \quad [7]$$

$$\frac{dZ_i}{dt} = \max\left(\gamma_i F_i - T_i, 0\right)\left(1 - 3Z_i + Z_i^2\right) \quad [8]$$

For all populations (basal and non-basal) the dynamics of the fraction of juveniles Z_i hence follows a separable function, consisting of a factor $\max\left(\gamma_i F_i - T_i, 0\right)$ that only depends on the total species densities C_i and a factor $\left(1 - 3Z_i + Z_i^2\right)$ that only depends on the fraction of juveniles Z_i. Irrespective of the fluctuations in the total species densities C_i, the fraction of juveniles in each population will therefore approach the unique root in the interval [0,1] of the quadratic condition $\left(1 - 3Z_i + Z_i^2\right) = 0$ for $t \to \infty$, i.e. approach the constant value:

$$\overline{Z} = \frac{3}{2} - \frac{1}{2}\sqrt{5} \approx 0.38 \quad [9]$$

In the long run the dynamics of this juvenile-adult abundance model are therefore captured by a model that only considers total species abundances:

$$\frac{dC_i}{dt} = \max\left(\gamma_i F_i - T_i, 0\right)(1-\overline{Z})C_i - \mu_i C_i - \sum_{k>i} \alpha_k \psi_{ki} \frac{C_k}{H_k + E_k} C_i \quad [10]$$

with E_i and F_i given by Eq. (5) and Eq. (6), respectively.

Computing eigenvalues of the stage-structured model. To verify the local stability of the community states that appear to be stable based on numerical simulations I compute the eigenvalues characterising the dynamics in the neighbourhood of the equilibrium using the Jacobian matrix. In the neighbourhood of an equilibrium of the stage-structured model persistence of a species in the community guarantees that starvation does not occur for the juveniles nor the adults. In such a close neighbourhood of an equilibrium state the reproduction and maturation rate of adult and juvenile consumers are therefore necessarily positive, such that

$$b_i(F_i) = \max\left((2-q)\gamma_i F_i - T_i, 0\right) = (2-q)\gamma_i F_i - T_i \quad [11]$$

$$m_i(F_i) = \max\left(q\gamma_i F_i - T_i, 0\right) = q\gamma_i F_i - T_i \quad [12]$$

The dynamics of the total species densities C_i and the fraction of juveniles in the populations Z_i can then be described by simplified versions of the ODEs. (3) and (4):

$$\begin{aligned}\frac{dC_i}{dt} &= \left((2-q)\gamma_i F_i - T_i\right)(1-Z_i)C_i - \mu_i C_i \\ &\quad - \left(\phi Z_i + (2-\phi)(1-Z_i)\right) C_i \sum_{k>i} \alpha_k \psi_{ki} \frac{\left(qZ_k + (2-q)(1-Z_k)\right) C_k}{H_k + E_k}\end{aligned} \quad [13]$$

$$\begin{aligned}\frac{dZ_i}{dt} &= \left((2-q)\gamma_i F_i - T_i\right)(1-Z_i)^2 - \left(q\gamma_i F_i - T_i\right) Z_i \\ &\quad -2(\phi-1)(1-Z_i)Z_i \sum_{k>i} \alpha_k \psi_{ki} \frac{\left(qZ_k + (2-q)(1-Z_k)\right) C_k}{H_k + E_k}\end{aligned} \quad [14]$$

The whole system of differential equations can be summarised as:

$$\frac{d\mathbf{C}}{dt} = \mathbf{K}\left(\mathbf{C}, \mathbf{Z}\right) \quad [15]$$

$$\frac{d\mathbf{Z}}{dt} = \mathbf{L}\left(\mathbf{C}, \mathbf{Z}\right) \quad [16]$$

in which $\mathbf{C}$ and $\mathbf{Z}$ are the vectors of total species abundances and fractions of juveniles in all populations, respectively. The vector-valued functions $\mathbf{K}(\mathbf{C}, \mathbf{Z})$ and $\mathbf{L}(\mathbf{C}, \mathbf{Z})$ contain the right-hand side of the ODEs dC_i/dt (13) and dZ_i/dt (14) for the species-density subsystem, respectively.

For a community with m species the Jacobian matrix of this model is a $2m \times 2m$ matrix $\mathbf{J}$ of the form:

$$\mathbf{J} = \begin{pmatrix} \dfrac{\partial \mathbf{K}}{\partial \mathbf{C}} & \dfrac{\partial \mathbf{K}}{\partial \mathbf{Z}} \\ \dfrac{\partial \mathbf{L}}{\partial \mathbf{C}} & \dfrac{\partial \mathbf{L}}{\partial \mathbf{Z}} \end{pmatrix} = \begin{pmatrix} \mathbf{V^1} + \mathbf{W^1} & \mathbf{V^2} + \mathbf{W^2} \\ \mathbf{V^3} + \mathbf{W^3} & \mathbf{V^4} + \mathbf{W^4} \end{pmatrix} \quad [17]$$

Each of the 4 parts of J is a $m \times m$ matrix containing the partial derivatives of the functions $\mathbf{K}(\mathbf{C}, \mathbf{Z})$ and $\mathbf{L}(\mathbf{C}, \mathbf{Z})$ with respect to the total species densities $(C_1, \ldots, C_m)$ and fractions of juveniles $(Z_1, \ldots, Z_m)$. $\mathbf{V^1}$, $\mathbf{V^2}$, $\mathbf{V^3}$ and $\mathbf{V^4}$ are 4 $m \times m$ matrices that capture the direct effects of two species in the community on each other, while $\mathbf{W^1}$, $\mathbf{W^2}$, $\mathbf{W^3}$ and $\mathbf{W^4}$ are 4 $m \times m$ matrices that capture the indirect effects between two species that operates through a third species. More specifically, indirect effects occur between species because changes in the total density C_j and the fraction of juveniles Z_j influence the encounter rate E_k of a consumer species k, which in turn affects the predation rate of species k on species i (last summation terms in ODEs above). Indirect effects hence involve interactions between a predator species k and two of its prey species with indices i and j.

The elements of the matrices $\mathbf{V^1}$, $\mathbf{V^2}$, $\mathbf{V^3}$ and $\mathbf{V^4}$ are defined as:

$$V^1_{i,j} = \frac{d}{dC_j}\left(dC_i/dt\right),\ V^2_{i,j} = \frac{d}{dZ_j}\left(dC_i/dt\right),\ V^3_{i,j} = \frac{d}{dC_j}\left(dZ_i/dt\right),\ V^4_{i,j} = \frac{d}{dZ_j}\left(dZ_i/dt\right)$$

Notice however that the derivatives with respect to C_j and Z_j in these expressions are evaluated while ignoring the indirect effects that will be captured by the matrices $\mathbf{W^1}$, $\mathbf{W^2}$, $\mathbf{W^3}$ and $\mathbf{W^4}$, that is, while treating the quantities E_k in the predation mortality terms (last summation terms in ODEs (13) and (14)) as constants.

The entries V^1_{ij} are given by:

$$V^1_{ij} = \begin{cases} \left((2-q)\gamma_1 \dfrac{\delta F_1^2}{P} - T_1\right)(1-Z_1) - \mu_1 \\ \quad -(\phi Z_1 + (2-\phi)(1-Z_1)) \displaystyle\sum_{k>1} \alpha_k \psi_{k1} \frac{(qZ_k + (2-q)(1-Z_k))\, C_k}{H_k + E_k} & i = j = 1 \\ ((2-q)\gamma_i F_i - T_i)(1-Z_i) - \mu_i \\ \quad -(\phi Z_i + (2-\phi)(1-Z_i)) \displaystyle\sum_{k>i} \alpha_k \psi_{ki} \frac{(qZ_k + (2-q)(1-Z_k))\, C_k}{H_k + E_k} & i = j \neq 1 \\ -\alpha_j \psi_{ji} \dfrac{(qZ_j + (2-q)(1-Z_j))}{H_j + E_j} (\phi Z_i + (2-\phi)(1-Z_i))\, C_i & i < j \\ (2-q)\gamma_i \dfrac{H_i}{(H_i+E_i)^2} \psi_{ij} (\phi Z_j + (2-\phi)(1-Z_j))(1-Z_i) C_i & i > j \end{cases} \quad [18]$$

In the above expressions for the matrix elements V^1_{ij} with $i > j$ I have used the identities

$$\frac{dF_i}{dC_j} = \frac{dF_i}{dE_i}\frac{dE_i}{dC_j} = \frac{H_i}{(H_i+E_i)^2}\frac{dE_i}{dC_j} = \frac{H_i}{(H_i+E_i)^2}\psi_{ij}\left(\phi Z_j + (2-\phi)(1-Z_j)\right)$$

and

$$\begin{aligned} \frac{d(F_1 C_1)}{dC_1} &= \frac{d}{dC_1}\frac{PC_1}{\delta + \alpha_1 (qZ_1 + (2-q)(1-Z_1))\, C_1} \\ &= \frac{\delta P}{(\delta + \alpha_1 (qZ_1 + (2-q)(1-Z_1))\, C_1)^2} \\ &= \frac{\delta F_1^2}{P} \end{aligned}$$

In an equilibrium state all per-capita growth rates $(dC_i/dt)/C_i$ vanish such that the entries of the matrix $\mathbf{V^1}$ simplify to:

$$V^1_{ij} = \begin{cases} (2-q)\gamma_1 \left(\dfrac{\delta F_1}{P} - 1\right) F_1 (1-Z_1) & i = j = 1 \\ 0 & i = j \neq 1 \\ -\alpha_j \psi_{ji} \dfrac{(qZ_j + (2-q)(1-Z_j))}{H_j + E_j} (\phi Z_i + (2-\phi)(1-Z_i))\, C_i & i < j \\ (2-q)\gamma_i \dfrac{H_i}{(H_i+E_i)^2} \psi_{ij} (\phi Z_j + (2-\phi)(1-Z_j))(1-Z_i) C_i & i > j \end{cases} \quad [19]$$

The entries V^2_{ij} are given by:

$$V^2_{ij} = \begin{cases} -\left((2-q)\gamma_1 \dfrac{(\delta + \alpha_1 q C_1) F_1^2}{P} - T_1\right) C_1 \\ \quad -2(\phi-1) C_1 \displaystyle\sum_{k>1} \alpha_k \psi_{k1} \frac{(qZ_k + (2-q)(1-Z_k))\, C_k}{H_k + E_k} & i = j = 1 \\ -((2-q)\gamma_i F_i - T_i)\, C_i \\ \quad -2(\phi-1) C_i \displaystyle\sum_{k>i} \alpha_k \psi_{ki} \frac{(qZ_k + (2-q)(1-Z_k))\, C_k}{H_k + E_k} & i = j \neq 1 \\ -\alpha_j \psi_{ji} \dfrac{2\,(q-1)\, C_j}{H_j + E_j} (\phi Z_i + (2-\phi)(1-Z_i))\, C_i & i < j \\ (2-q)\gamma_i \dfrac{H_i}{(H_i+E_i)^2} \psi_{ij} 2\,(\phi-1)\, C_j (1-Z_i) C_i & i > j \end{cases} \quad [20]$$

To derive the expressions for the matrix elements V^2_{ij} with $i > j$ I have used the identities

$$\frac{dF_i}{dZ_j} = \frac{dF_i}{dE_i}\frac{dE_i}{dZ_j} = \frac{H_i}{(H_i+E_i)^2}\frac{dE_i}{dZ_j} = \frac{H_i}{(H_i+E_i)^2}\psi_{ij} 2\,(\phi-1)\, C_j$$

and

$$\begin{aligned}\frac{d(F_1(1-Z_1))}{dZ_1} &= \frac{d}{dZ_1}\frac{P(1-Z_1)}{\delta+\alpha_1\left(qZ_1+(2-q)(1-Z_1)\right)C_1}\\ &= -\frac{\left(\delta+\alpha_1 qC_1\right)P}{\left(\delta+\alpha_1\left(qZ_1+(2-q)(1-Z_1)\right)C_1\right)^2}\\ &= -\frac{\left(\delta+\alpha_1 qC_1\right)F_1^2}{P}\end{aligned}$$

The entries V_{ij}^3 are given by:

$$V_{ij}^3 = \begin{cases} -\gamma_1\frac{\alpha_1\left(qZ_1+(2-q)(1-Z_1)\right)F_1^2}{P}\left((2-q)(1-Z_1)^2-qZ_1\right) & i=j=1\\ 0 & i=j\neq 1\\ -\alpha_j\psi_{ji}\frac{(qZ_j+(2-q)(1-Z_j))}{H_j+E_j}2(\phi-1)(1-Z_i)Z_i & i<j\\ \gamma_i\frac{H_i}{(H_i+E_i)^2}\psi_{ij}\left(\phi Z_j+(2-\phi)(1-Z_j)\right)\left((2-q)(1-Z_i)^2-qZ_i\right) & i>j\end{cases} \quad [21]$$

To derive the expressions for the matrix elements V_{ij}^3 with $i=j=1$ I have used the identity

$$\begin{aligned}\frac{dF_1}{dC_1} &= \frac{d}{dC_1}\frac{P}{\delta+\alpha_1\left(qZ_1+(2-q)(1-Z_1)\right)C_1}\\ &= -\frac{\alpha_1\left(qZ_1+(2-q)(1-Z_1)\right)P}{\left(\delta+\alpha_1\left(qZ_1+(2-q)(1-Z_1)\right)C_1\right)^2}\\ &= -\frac{\alpha_1\left(qZ_1+(2-q)(1-Z_1)\right)F_1^2}{P}\end{aligned}$$

Finally, the entries V_{ij}^4 are given by:

$$V_{ij}^4 = \begin{cases} -\gamma_1\frac{2\alpha_1(q-1)C_1F_1^2}{P}\left((2-q)(1-Z_1)^2-qZ_1\right)\\ -2\left((2-q)\gamma_1F_1-T_1\right)(1-Z_1)-(q\gamma_1F_1-T_1)\\ -2(\phi-1)(1-2Z_1)\sum_{k>1}\alpha_k\psi_{k1}\frac{(qZ_k+(2-q)(1-Z_k))C_k}{H_k+E_k} & i=j=1\\ -2\left((2-q)\gamma_iF_i-T_i\right)(1-Z_i)-(q\gamma_iF_i-T_i)\\ -2(\phi-1)(1-2Z_i)\sum_{k>i}\alpha_k\psi_{ki}\frac{(qZ_k+(2-q)(1-Z_k))C_k}{H_k+E_k} & i=j\neq 1\\ -\alpha_j\psi_{ji}\frac{2(q-1)C_j}{H_j+E_j}2(\phi-1)(1-Z_i)Z_i & i<j\\ \gamma_i\frac{H_i\psi_{ij}2(\phi-1)C_j}{(H_i+E_i)^2}\left((2-q)(1-Z_i)^2-qZ_i\right) & i>j\end{cases} \quad [22]$$

The derivation of the expressions for the matrix elements V_{ij}^4 with $i=j=1$ is based on the identity

$$\begin{aligned}\frac{dF_1}{dZ_1} &= \frac{d}{dZ_1}\frac{P}{\delta+\alpha_1\left(qZ_1+(2-q)(1-Z_1)\right)C_1}\\ &= -\frac{2\alpha_1(q-1)C_1P}{\left(\delta+\alpha_1\left(qZ_1+(2-q)(1-Z_1)\right)C_1\right)^2}\\ &= -\frac{2\alpha_1(q-1)C_1F_1^2}{P}\end{aligned}$$

As explained above, indirect effects occur between species because changes in the total density C_j and fraction of juveniles Z_j influence the encounter rate E_k of a consumer species k, which in turn affects the predation rate of species k on species i.

These indirect effects therefore always arise because of the summation terms representing predation mortality in eqs. (13) and (14). In the predation rate of species k only the term $1/(H_k + E_k)$ depends on the total density C_j and the fraction of juveniles Z_j of species j and the derivatives of this term with respect to C_j and Z_j equal

$$-\frac{1}{(H_k + E_k)^2}\psi_{kj}\left(\phi Z_j + (2-\phi)(1-Z_j)\right)$$

and

$$-\frac{1}{(H_k + E_k)^2}\psi_{kj} 2\left(\phi - 1\right) C_j$$

respectively. The elements of the matrices $\mathbf{W^1}$, $\mathbf{W^2}$, $\mathbf{W^3}$ and $\mathbf{W^4}$ are hence defined as:

$$W^1_{i,j} = \left(\phi Z_i + (2-\phi)(1-Z_i)\right) C_i \left(\phi Z_j + (2-\phi)(1-Z_j)\right) \sum_{k>i} \alpha_k \psi_{ki} \psi_{kj} \frac{\left(qZ_k + (2-q)(1-Z_k)\right) C_k}{(H_k + E_k)^2}$$

$$W^2_{i,j} = \left(\phi Z_i + (2-\phi)(1-Z_i)\right) C_i \, 2(\phi-1) C_j \sum_{k>i} \alpha_k \psi_{ki} \psi_{kj} \frac{\left(qZ_k + (2-q)(1-Z_k)\right) C_k}{(H_k + E_k)^2}$$

$$W^3_{i,j} = 2(\phi-1)(1-Z_i) Z_i \left(\phi Z_j + (2-\phi)(1-Z_j)\right) \sum_{k>i} \alpha_k \psi_{ki} \psi_{kj} \frac{\left(qZ_k + (2-q)(1-Z_k)\right) C_k}{(H_k + E_k)^2}$$

$$W^4_{i,j} = 2(\phi-1)(1-Z_i) Z_i \, 2(\phi-1) C_j \sum_{k>i} \alpha_k \psi_{ki} \psi_{kj} \frac{\left(qZ_k + (2-q)(1-Z_k)\right) C_k}{(H_k + E_k)^2}$$

Note that i and j may be equal to each other as changes in the total density of C_i and the fraction of juveniles Z_i change the predation rate of species k on species i through a change in the functional response of species k, which effect is not captured by the matrices $\mathbf{V^1}$, $\mathbf{V^2}$, $\mathbf{V^3}$ and $\mathbf{V^4}$. Furthermore, note that all elements W^1_{ij} are positive for species that are exposed to predation and equal to 0 only for top predators. Together with the fact that $V^1_{ii} = 0$ for $i \neq 0$ this implies that the effect of species density C_i on its own rate of change dC_i/dt is 0 for top predators and positive for all non-basal species experiencing predation.

All communities resulting from the stage-structured model with asymmetry in feeding and predation between juveniles and adults ($q = 0.7$, $\phi = 1.8$) for which the minimum and maximum values of the total species density differed less than 10^{-6} from each other for all species were considered stable. All communities for which the minimum and maximum values of total species density differed more than 10^{-6} from each other for at least 1 species, were considered unstable (cycling) communities. For both stable and unstable communities the average total abundance and fraction of juveniles observed in the simulation were used as starting values to numerically solve for the equilibrium state using the package 'rootSolve' (1, 2) in R (3). For all 115 stable communities the equilibrium community state was successfully located and was numerically indistinguishable from the average densities and juvenile fractions observed in the numerical simulations. For 147 communities that were considered unstable (cycling) the numerical solution procedure also converged to an equilibrium community state with all species present, while for 238 unstable communities the numerical solution procedure did not converge to such an equilibrium state.

For all communities, for which the equilibrium state was successfully located, the Jacobian matrix J was evaluated by substituting for all species the equilibrium values for the total abundance and fraction of juveniles as well as all general and species-specific parameters into the matrices $\mathbf{V^1}$, $\mathbf{V^2}$, $\mathbf{V^3}$, $\mathbf{V^4}$, $\mathbf{W^1}$, $\mathbf{W^2}$, $\mathbf{W^3}$ and $\mathbf{W^4}$. The eigenvalues of the Jacobian matrix $\mathbf{J}$ (see Eq. (17)) were subsequently computed numerically using the routine eigen() in R (3). These calculations of the Jacobian matrix based on the analytical expressions for the matrices $\mathbf{V^1}$, $\mathbf{V^2}$, $\mathbf{V^3}$, $\mathbf{V^4}$, $\mathbf{W^1}$, $\mathbf{W^2}$, $\mathbf{W^3}$ and $\mathbf{W^4}$ were verified by also computing the Jacobian matrix numerically using central differencing methods applied to the right-hand side of the ODEs (13) and (14) for dC_i/dt and dZ_i/dt.

For both stable and unstable communities the largest real part among the eigenvalues (i.e. the real part of the dominant eigenvalue) is shown in Fig. S4. For stable communities this real part was always negative, ranging between -0.061 and $-9.8 \cdot 10^{-5}$. For unstable communities this real part was always positive, ranging between $1.3 \cdot 10^{-4}$ and 0.124.

Sources of community stability. For stable communities the effect of dynamic changes in population stage-structure (i.e. changes in the juvenile-adult ratio) on the stability of the community equilibrium was evaluated further. The dominant eigenvalues computed for these communities were compared with the eigenvalues of the top-left submatrix of J, that is the $m \times m$ matrix $\partial\mathbf{K}/\partial\mathbf{C}$ of these communities. The latter matrix determines the stability of the species-density subsystem on its own with the juvenile fraction of each species equal to its equilibrium value. More specifically, this reduced model of the species-density subsystem on its own is described by the same dynamic equations for the total species densities as in the full model (Eq. (13)), but with the fraction of juveniles Z_i in the populations taken constant over time and equal to the fraction of juveniles of the

species at equilibrium $\tilde{Z}_i$:

$$\frac{dC_i}{dt} = ((2-q)\gamma_i F_i - T_i)\,(1-\tilde{Z}_i)C_i - \mu_i C_i$$
$$- \sum_{k>i} \alpha_k \psi_{ki} \frac{\left(\phi\tilde{Z}_i + (2-\phi)(1-\tilde{Z}_i)\right) C_i}{H_k + E_k} \left(q\tilde{Z}_k + (2-q)(1-\tilde{Z}_k)\right) C_k \quad [23]$$

Comparing the eigenvalues of this reduced model with the eigenvalues of the full model, in which the juvenile fraction in the population Z_i is dynamic and changes at the same time scale as the total species density, reveals the impact of dynamic changes in the population structure of the species on the stability of the community equilibrium. The eigenvalues of the reduced model can be computed from its Jacobian matrix which equals the matrix $\partial\mathbf{K}/\partial\mathbf{C} = \mathbf{V^1} + \mathbf{W^1}$. This matrix corresponds to the community matrix with elements $\partial(dC_i/dt)/\partial C_j$ that captures the per-capita effect of the species in the community on each other's growth rate and determines stability in community models without population structure.

To further assess the differences between constant and a dynamic juvenile fraction in the population, for all stable communities resulting from the stage-structured model with asymmetry in feeding and predation between juveniles and adults ($q = 0.7$, $\phi = 1.8$) community dynamics were computed starting from the equilibrium community state using the reduced model including the differential equations dC_i/dt for the species-density subsystem only (Eq. (23)), with the juvenile faction Z_i in each of the populations taken equal to its equilibrium value inferred from the stable community state (see Fig. 4C, top-left panel, in the main text and Fig. S6). Similarly, community dynamics were computed with an age-structured analogue of the full model. This age-structured model includes differential equations dC_i/dt for the species-density subsystem and dZ_i/dt for the species-structure subsystem, but substitutes the juvenile maturation rate $m_i(F_i)$ for each of the species in the community with a constant value. This constant value is equal to the maturation rate that juveniles of the species experience in the community equilibrium and is indicated with $\tilde{m}_i$. Dynamics are then described by the equations:

$$\frac{dC_i}{dt} = b_i(F_i)(1-Z_i)C_i - \mu_i C_i$$
$$- (\phi Z_i + (2-\phi)(1-Z_i))\, C_i \sum_{k>i} \alpha_k \psi_{ki} \frac{(qZ_k + (2-q)(1-Z_k))\, C_k}{H_k + E_k} \quad [24]$$

$$\frac{dZ_i}{dt} = b_i(F_i)(1-Z_i)^2 - \tilde{m}_i Z_i$$
$$-2(\phi-1)(1-Z_i)Z_i \sum_{k>i} \alpha_k \psi_{ki} \frac{(qZ_k + (2-q)(1-Z_k))\, C_k}{H_k + E_k} \quad [25]$$

The simulations with this age-structured analogue were also started from the equilibrium community state (see Fig. 4C, top-right panel, in the main text and Fig. S6). For comparison, community dynamics were also computed with the full model including the differential equations dC_i/dt for the species-density subsystem (Eq. (3)) and dZ_i/dt for the species-structure subsystem (Eq. (4)) starting from a community state in which the initial density of each species was exactly 50% of its equilibrium value inferred from the stable community state (see Fig. 4C, bottom panel in the main text and Fig. S6).

Extent of self-regulation. For stable communities the extent of self-regulation of species is assessed with the diagonal elements of the community matrix, the $m \times m$ matrix $\partial\mathbf{K}/\partial\mathbf{C}$ (Eq. (17)), which measures the positive or negative effect of the total species abundance C_i on its own rate of change dC_i/dt (Fig. S5).

Stage-structured biomass model of species dynamics

To check the robustness of the results obtained with the stage-structured model in terms of juvenile and adult numerical densities, numerical simulations of community dynamics were also carried out, using a stage-structured biomass model for species dynamics (4). More specifically, each species was represented by 3 life history stages, referred to as juveniles, subadults and adults. Such a stage-structured biomass model (4) constitutes an approximation to a size-structured population model that accounts for a complete size distribution of individuals between their size at birth and size at maturation, in which the rates of feeding, metabolic maintenance, somatic growth, and reproduction all scale linearly with individual body size (5). Juvenile and subadult individuals are assumed to use their net-energy production (the difference between assimilation and metabolic maintenance rate) for somatic growth, whereas adults are assumed not to grow and use their net-energy production for reproduction. Dynamics are in terms of juvenile, subadult and adult biomass densities, indicated with J_i, S_i and A_i, respectively.

In the absence of predation the life history processes in the stage-structured biomass model are described by the following

mass-specific rate functions:

$$\text{Juvenile somatic growth} \quad g_i^J(F_i) = \max\left((2-q)\gamma_i F_i - T_i, 0\right) \quad [26]$$

$$\text{Subadult somatic growth} \quad g_i^S(F_i) = \max\left(q\gamma_i F_i - T_i, 0\right) \quad [27]$$

$$\text{Adult reproduction} \quad b_i(F_i) = \max\left((2-q)\gamma_i F_i - T_i, 0\right) \quad [28]$$

$$\text{Juvenile mortality} \quad d_i^J(F_i) = \mu_i - \min\left((2-q)\gamma_i F_i - T_i, 0\right) \quad [29]$$

$$\text{Subadult mortality} \quad d_i^S(F_i) = \mu_i - \min\left(q\gamma_i F_i - T_i, 0\right) \quad [30]$$

$$\text{Adult mortality} \quad d_i^A(F_i) = \mu_i - \min\left((2-q)\gamma_i F_i - T_i, 0\right) \quad [31]$$

$$\text{Juvenile maturation} \quad m_i^J(F_i) = \begin{cases} \dfrac{g_i^J(F_i) - D_i^J}{1 - z^{1-D_i^J/g_i^J(F_i)}} & \text{if } g_i^J(F_i) > 0 \\ 0 & \text{otherwise} \end{cases} \quad [32]$$

$$\text{Subadult maturation} \quad m_i^S(F_i) = \begin{cases} \dfrac{g_i^S(F_i) - D_i^S}{1 - z^{1-D_i^S/g_i^S(F_i)}} & \text{if } g_i^S(F_i) > 0 \\ 0 & \text{otherwise} \end{cases} \quad [33]$$

In these equations F_i represents the functional response of species i, which for the basal species equals:

$$F_1 = \frac{P}{\delta + \alpha_1\left((2-q)\,J_1 + q\,S_1 + (2-q)\,A_1\right)} \quad [34]$$

The parameter q in this expression determines the asymmetry in feeding capacity between juveniles, subadults and adults (for the purpose of this study taken the same for all species). Non-basal species forage following a type II functional response:

$$F_i = \frac{E_i}{H_i + E_i} \quad [35]$$

in which E_i represents the encounter rate of non-basal species i with prey biomass:

$$E_i = \sum_{k<i} \psi_{ik}\left(\phi\,J_k + (2-\phi)\,S_k + (2-\phi)\,A_k\right) \quad [36]$$

The parameter ϕ represents the bias of the consumer species toward feeding on juvenile as opposed to subadult and adult prey (for the purpose of this study taken the same for all species). Notice that all species are ordered according to their body size and hence species i can only feed on species with an index $k < i$.

The parameter T_i in the life history functions (26)-(33) represents the (mass-specific) loss rate through metabolic maintenance requirements, while the parameter μ_i represents the background mortality. The parameter γ_i determines the maximum assimilation rate per unit biomass, while the parameter z equals the ratio between the body size at entering and leaving each of the immature stages (the juvenile and subadult stage). The parameters γ_i, q and T_i also determine the minimum food availability that is needed by juveniles, subadults and adults to just keep itself alive without producing any offspring and without maturing.

D_i^J and D_i^S indicate the total mortality rate experienced by juvenile and subadult individuals, respectively, which in the absence of predation equals μ_i, but in the presence of predation also includes the predation mortality (see below; note that D_i^J and D_i^S do not include starvation mortality as starvation mortality only occurs when $g_i^J(F_i) = 0$ or $g_i^S(F_i) = 0$, in which case $m_i^J(F_i) = 0$ and $m_i^S(F_i) = 0$, respectively). Equations (28), (26), (27), (32) and (33) express that adult reproduction, juvenile and subadult growth in body size and juvenile and subadult maturation come to a halt under starvation conditions, which for juveniles, subadults and adults occur when $(2-q)\gamma_i F_i < T_i$, $q\gamma_i F_i < T_i$ and $(2-q)\gamma_i F_i < T_i$, respectively. Under these starvation conditions juveniles, subadults and adults experience increased mortality (Eqs. (29), (30) and (31)). The mass-specific juvenile and subadult maturation rates depends on both juvenile and subadult growth rate in body size as well as total juvenile and subadult mortality, D_i^J and D_i^S, respectively. The functional form of the maturation rates $m_i^J(F_i)$ and $m_i^S(F_i)$ is chosen such that any equilibrium state predicted by the stage-structured biomass model corresponds uniquely to an equilibrium state of a structured model that accounts for a complete size distribution of individuals between their size at birth and size at maturation, in which the rates of feeding, metabolic maintenance, somatic growth, and reproduction all scale linearly with individual body size (5).

A representation of each species by 3 life history stages with the smallest juveniles most vulnerable to predation mortality and the maturation of the larger immature individuals limited most by food availability was chosen because the dynamics of such a 3-stage biomass model has been found to closely resemble the dynamics of population models with a complete size distribution that are based on a dynamic energy budget model for the individual energetics (6). Similar results as presented in Fig. S7, S8 and S9 have, however, also been obtained using a stage-structured biomass model with only a single juvenile and adult life history stage to describe species dynamics.

The dynamics of the juvenile, subadult and adult biomass densities of all species in the community are now described by the following set of ordinary differential equations (ODEs):

$$\frac{dJ_i}{dt} = b_i(F_i)A_i + g_i^J(F_i)J_i - m_i^J(F_i)J_i - d_i^J(F_i)J_i - \phi J_i \sum_{k>i} \alpha_k \psi_{ki} \frac{(2-q)J_k + qS_k + (2-q)A_k}{H_k + E_k} \quad [37]$$

$$\frac{dS_i}{dt} = m_i^J(F_i)J_i + g_i^S(F_i)S_i - m_i^S(F_i)S_i - d_i^S(F_i)S_i - (2-\phi)S_i \sum_{k>i} \alpha_k \psi_{ki} \frac{(2-q)J_k + qS_k + (2-q)A_k}{H_k + E_k} \quad [38]$$

$$\frac{dA_i}{dt} = m_i^S(F_i)S_i - d_i^A(F_i)A_i - (2-\phi)A_i \sum_{k>i} \alpha_k \psi_{ki} \frac{(2-q)J_k + qS_k + (2-q)A_k}{H_k + E_k} \quad [39]$$

In these equations E_k and H_k represent the encounter rate with prey and the half-saturation density in the functional response of species k, respectively (Eq. (36)), while the parameters q and ϕ represent the asymmetry in foraging rate and predation risk, respectively, between juvenile, subadult and adult individuals. The default values for these parameters equal 1, implying that all 3 stages have identical life history rates ($q = 1$) and that consumers feed indiscriminately on juveniles, subadults and adults of their prey species ($\phi = 1$). Finally, the parameter α_k represents the maximum (mass-specific) foraging rate of consumer species k.

Given the above equations, the total juvenile mortality rate, on which the maturation rate (Eq. (32)) of juvenile into subadult biomass depends, is the sum of background (but not starvation) mortality and predation mortality:

$$D_i^J = \mu_i + \phi \sum_{k>i} \alpha_k \psi_{ki} \frac{(2-q)J_k + qS_k + (2-q)A_k}{H_k + E_k} \quad [40]$$

Starvation mortality is excluded from D_i^J because the maturation rate equals 0 under starvation conditions. Analogously, the total subadult mortality rate, on which the maturation rate (Eq. (33)) of subadult into adult biomass depends, is the sum of background (but not starvation) mortality and predation mortality:

$$D_i^S = \mu_i + (2-\phi) \sum_{k>i} \alpha_k \psi_{ki} \frac{(2-q)J_k + qS_k + (2-q)A_k}{H_k + E_k} \quad [41]$$

Model parameterisation and numerical simulation details. Parameterisation of the stage-structured biomass model follows the same procedure as the stage-structured model in terms of juvenile and adult abundance (see Materials and Methods). In short, half-saturation prey densities H_i for non-basal species are sampled from a uniform distribution on the interval $[0.5, 2.5]$. The ratio between the smallest and the largest body size in each of the two immature life stages, z, that occurs in the maturation rates of the stage-structured biomass model (Eq. (32)) and (Eq. (33)), is for all species taken the same and equal to $z = 0.1$. Individuals are hence assumed to grow 2 orders of magnitude in body size between birth and maturation. The parameters α_i, γ_i, T_i and μ_i all represent (mass-specific) rates and are assumed to scale with $w_i^{-0.25}$ following the equations:

$$\alpha_i = \alpha_0 \left(1 + 2\sigma_\alpha \left(x_{i1} - \tfrac{1}{2}\right)\right) w_i^{-0.25} \quad [42]$$

$$\gamma_i = \gamma_0 \left(1 + 2\sigma_\gamma \left(x_{i2} - \tfrac{1}{2}\right)\right) w_i^{-0.25} \quad [43]$$

$$T_i = T_0 \left(1 + 2\sigma_T \left(x_{i3} - \tfrac{1}{2}\right)\right) w_i^{-0.25} \quad [44]$$

$$\mu_i = \mu_0 \left(1 + 2\sigma_\mu \left(x_{i4} - \tfrac{1}{2}\right)\right) w_i^{-0.25} \quad [45]$$

The default mean values of the species-specific parameters equal $\alpha_0 = 1.0$, $\gamma_0 = 0.6$, $T_0 = 0.1$ and $\mu_0 = 0.015$ (6), while the species-specific parameters α_i, γ_i, T_i and μ_i are randomly selected from a Bates distribution of degree 3 around these mean values. A Bates distribution is the continuous probability distribution of the mean, X, of 3 independent uniformly distributed random variables on the unit interval. Random values from this distribution range between 0 and 1 with mean value of 1/2 and are easily generated by taking the mean of 3 independent samplings from a uniform distribution on the unit interval $[0, 1]$. The quantities x_{ij} are independent realisations of the random variable X, while σ_α, σ_γ, σ_T and σ_μ represent the one-sided, relative width of the distributions of the species-specific parameters α_i, γ_i, T_i and μ_i, respectively, around the mean values $\alpha_0 = 1.0$, $\gamma_0 = 0.6$, $T_0 = 0.1$ and $\mu_0 = 0.015$. Default values for these relative widths equal 0.1, such that all species-specific parameters α_i, γ_i, T_i and μ_i range between 0.9 and 1.1 times their default mean value and follow hump-shaped distributions within these ranges. The productivity P and turn-over rate δ of the exclusive resource of the basal species are taken equal to 60 and 2.0, respectively, in all computations. The two remaining parameters, the foraging asymmetry parameter q and the predation asymmetry parameter ϕ, in the model are varied between the different computations to assess their effect on community dynamics.

As described in the Materials and Methods section food webs are generated by selecting $N = 500$ random niche values n_i uniformly from the interval $[0, 1]$ and associated with species body mass following $w_i = (w_{max})^{n_i}(w_{min})^{(1-n_i)}$. Subsequently, the network of feeding interactions between these $N = 500$ species is constructed by generating for each non-basal species the midpoint of its feeding niche c_i following the procedure and default values for the mean prey-predator body mass ratio

described in the Materials and Methods and Fig. S10. Numerical integrations of the food web with $N = 500$ species are carried out using an adaptive Runge-Kutta (Cash-Karp) method implemented in C. Relative and absolute tolerances during the integration equal $1.0 \cdot 10^{-7}$ and $1.0 \cdot 10^{-13}$, respectively. During the first 10^4 time units no species are removed from the community, even if they attain very low density. For $t > 10^4$ each species, whose total biomass density $J_i + S_i + A_i$ drops below 10^{-8}, is removed from the community. This persistence threshold ensures that the product of the relative tolerance (10^{-7}) and the lowest species density (10^{-8}) is larger than the machine precision (equal to $1.11 \cdot 10^{-16}$ according to the IEEE 754-2008 standard in case of double precision). During numerical computations mean and variance as well as the maximum and minimum value of the total species biomass $J_i + S_i + A_i$ are continuously monitored for all species. The values of these measured statistics are reset whenever the community structure changes as one or more species in the community go extinct. Numerical integrations are halted whenever the community structure has not changed for 10^6 time units and no change has occurred from one time unit to the next in the values of these statistics (mean, minimum, maximum and variance of total species density) for all species in the community.

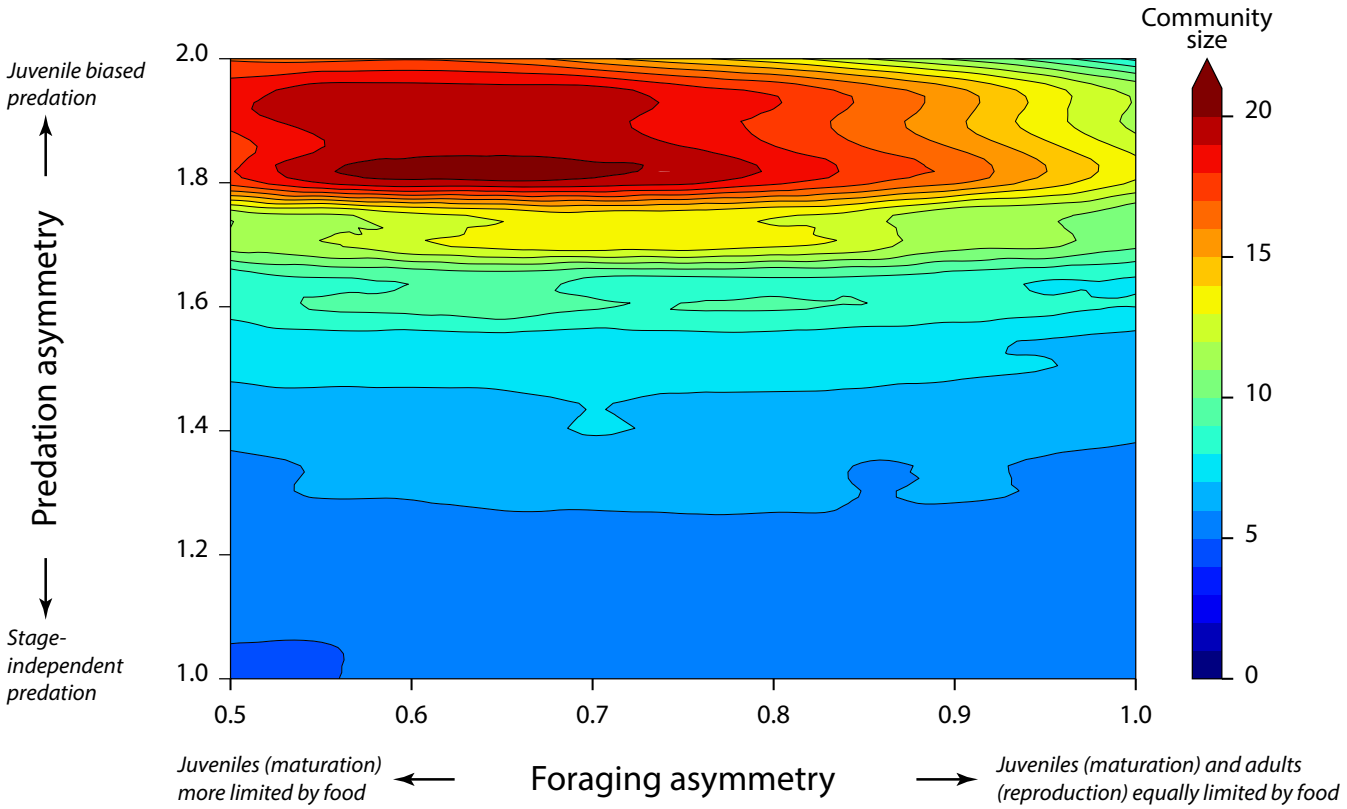

Fig. S1. Juvenile-adult asymmetry increases community diversity – Mean community size (non-basal species only) of 500 replicate food web simulations with juvenile-adult stage-structure for different values of foraging (q) and predation (ϕ) asymmetry between juveniles and adults. Larger communities result when predation is stronger on juveniles than on adults and maturation is more limited by food availability than reproduction.

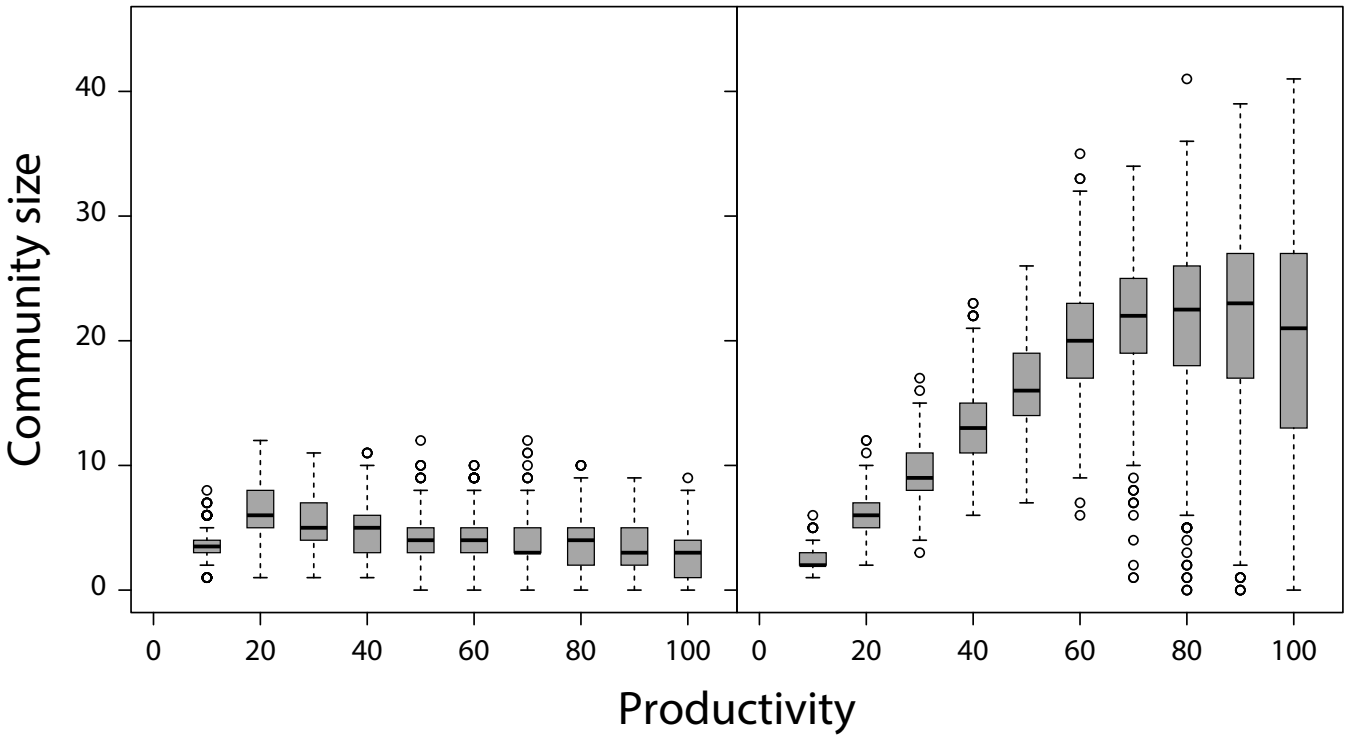

Fig. S2. Juvenile-adult asymmetry increases community diversity at all productivities – Boxplot of community sizes at different levels of system productivity P resulting from 500 replicate food web simulations without (*left*) and with stage-structure and foraging and predation asymmetry between juveniles and adults (*right*; $q = 0.7$, $\phi = 1.8$, see Materials and Methods).

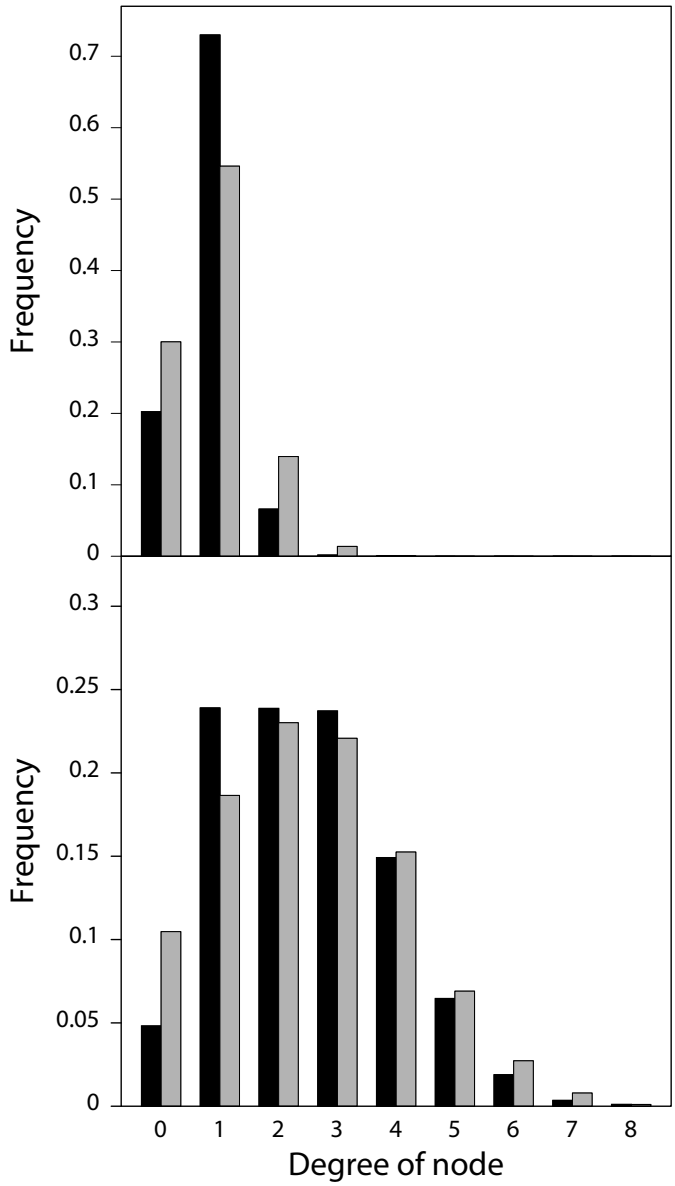

Fig. S3. Juvenile-adult asymmetry increases food web connectivity – Number of prey species (black bars; incoming network node links) and predators (grey bars; outgoing network node links) for all species in food webs resulting from 500 replicate simulations without (top panel) and with stage-structure and foraging and predation asymmetry between juveniles and adults (bottom panel; $q = 0.7$, $\phi = 1.8$).

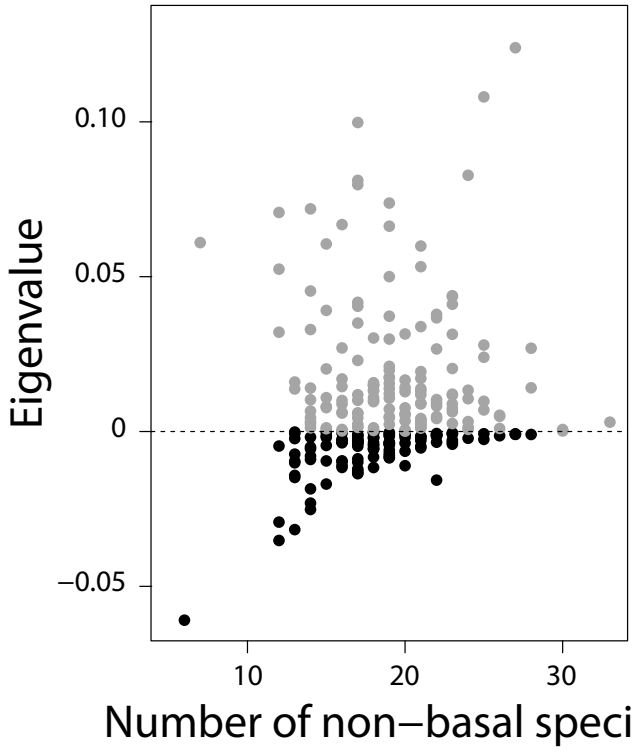

Fig. S4. Eigenvalues of the Jacobian matrix with largest real part determining community stability – Real part of the dominant (right-most) eigenvalue of the Jacobian matrix determining community stability as a function of community size for all stable communities (black dots) and all unstable communities for which the equilibrium could be solved for numerically (grey symbols) for the stage-structured model in case of foraging and predation asymmetry between juveniles and adults ($q = 0.7$, $\phi = 1.8$).

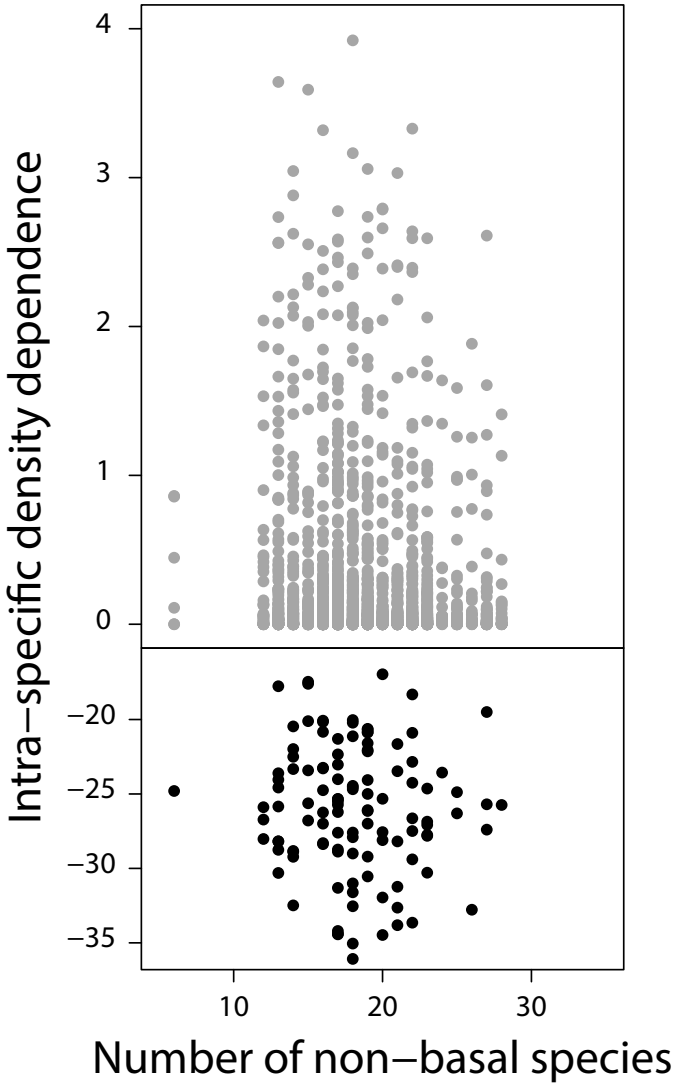

Fig. S5. Juvenile-adult asymmetry stabilises community dynamics without self-regulation – Strength of intra-specific density dependence for basal (*bottom*) and all non-basal species (*top*) in stable communities resulting from food web simulations with the stage-structured model and foraging and predation asymmetry between juveniles and adults ($q = 0.7, \phi = 1.8$). Intra-specific density dependence is assessed with the diagonal elements of the community matrix, which measures for basal and non-basal species the negative and positive effect, respectively, of total species abundance on its own rate of change (see Materials and Methods).

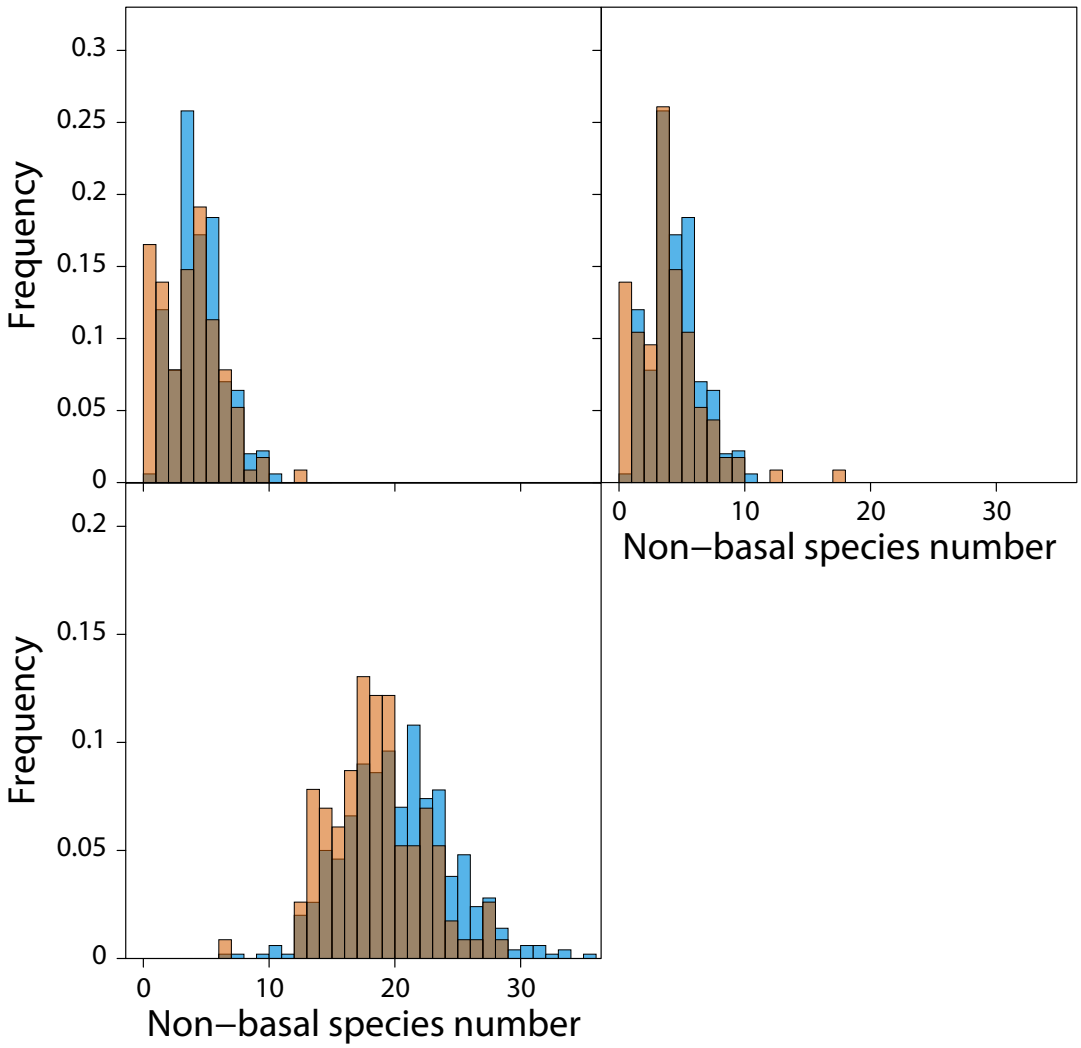

Fig. S6. Dynamic juvenile-adult ratio enforces complex community stability – Frequency distribution of community sizes (non-basal species only; red bars) resulting from simulations of dynamics for all stable communities generated by the stage-structured model in case of foraging and predation asymmetry between juveniles and adults ($q = 0.7$, $\phi = 1.8$) with different model variants (see Materials and Methods and section *Sources of community stability* above). Top-left panel shows results of the species-density subsystem on its own with the juvenile-adult ratio for each species constant in time and equal to its equilibrium value when initial species densities are identical to their equilibrium values. Top-right panel shows results of the coupled species-density and species-structure subsystem with the juvenile maturation rate for each species constant in time and equal to its equilibrium value when initial species densities are identical to their equilibrium values (These results represent dynamics of an analogous age-structured model). Bottom panel shows results of the coupled species-density and species-structure subsystem when initial densities for each species are reduced to 50% of their equilibrium densities. For reference, top and bottom panels also show the frequency distribution of community sizes (non-basal species only; blue bars) resulting from 500 replicate food web simulations without and with stage-structure and foraging and predation asymmetry between juveniles and adults, respectively, that are also presented in Figure 2 in the main text.

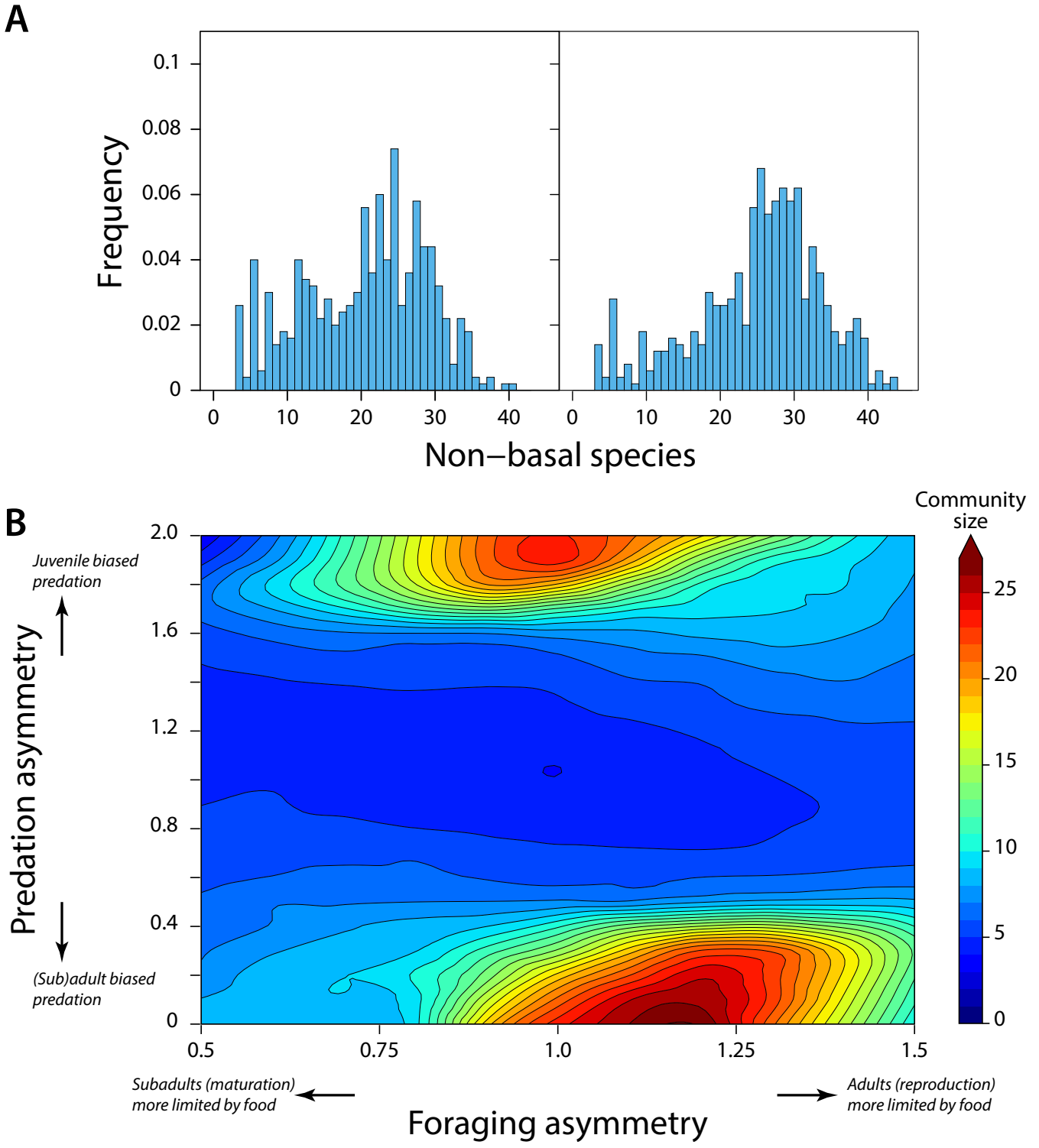

Fig. S7. Juvenile-adult asymmetry in biomass dynamics increases community diversity – *A*: Frequency distribution of community sizes (non-basal species only) resulting from 500 replicate food web simulations using the 3-stage biomass model including juveniles, subadults and adults (see section *Stage-structured biomass model of species dynamics* above) when juveniles are most vulnerable to predation and subadults are limited most by food availability (left panel; $q = 0.9$, $\phi = 1.8$) and when subadults and adults are more vulnerable to predation and small juveniles and adults are limited most by food availability (right panel; $q = 1.2$, $\phi = 0.2$). *B*: Mean community size (non-basal species only) of 500 replicate food web simulations using the 3-stage biomass model including juveniles, subadults and adults for different values of foraging (q) and predation (ϕ) asymmetry.

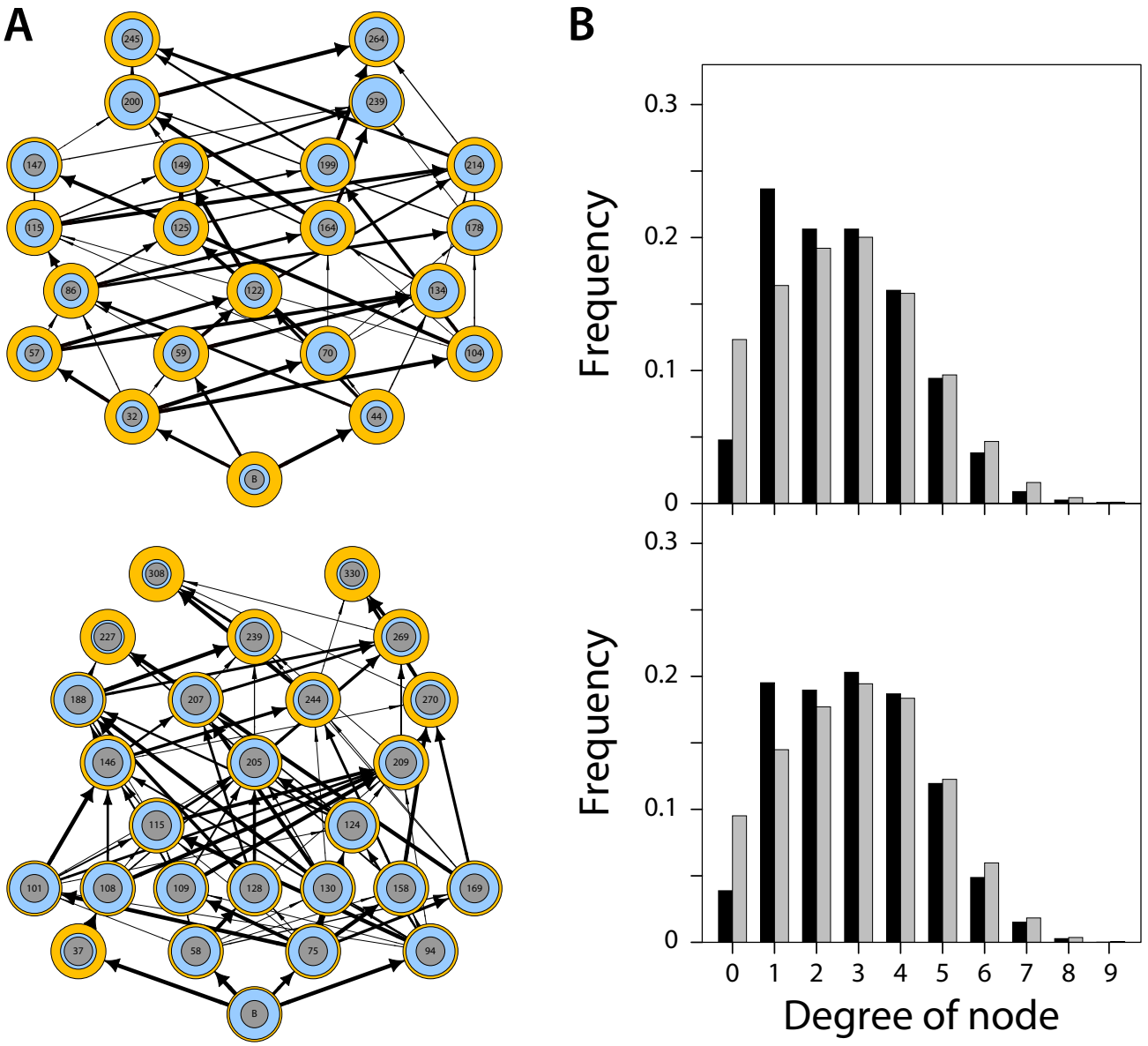

Fig. S8. Juvenile-adult asymmetry in biomass dynamics increases food web complexity – *A*: Examples of food webs resulting from simulations using the 3-stage biomass model including juveniles, subadults and adults (see *Stage-structured biomass model of species dynamics* above) when juveniles are more vulnerable to predation and subadults are limited most by food availability (top panel; $q = 0.9$, $\phi = 1.8$) and when subadults and adults are more vulnerable to predation and small juveniles and adults are limited most by food availability (bottom panel; $q = 1.2$, $\phi = 0.2$). Vertical position indicates trophic level. Inner circles indicate the biomass fraction of juveniles (grey) and total immatures (blue) in the population. Arrow widths indicate the relative feeding preference (ψ_{ik}, see Materials and Methods) of consumers for a particular prey species. *B*: Number of prey species (black bars; incoming network node links) and predators (grey bars; outgoing network node links) for all species in food webs resulting from 500 replicate simulations using the 3-stage biomass model including juveniles, subadults and adults when juveniles are more vulnerable to predation and subadults are limited most by food availability (top panel; $q = 0.9$, $\phi = 1.8$) and when subadults and adults are more vulnerable to predation and small juveniles and adults are limited most by food availability (bottom panel; $q = 1.2$, $\phi = 0.2$).

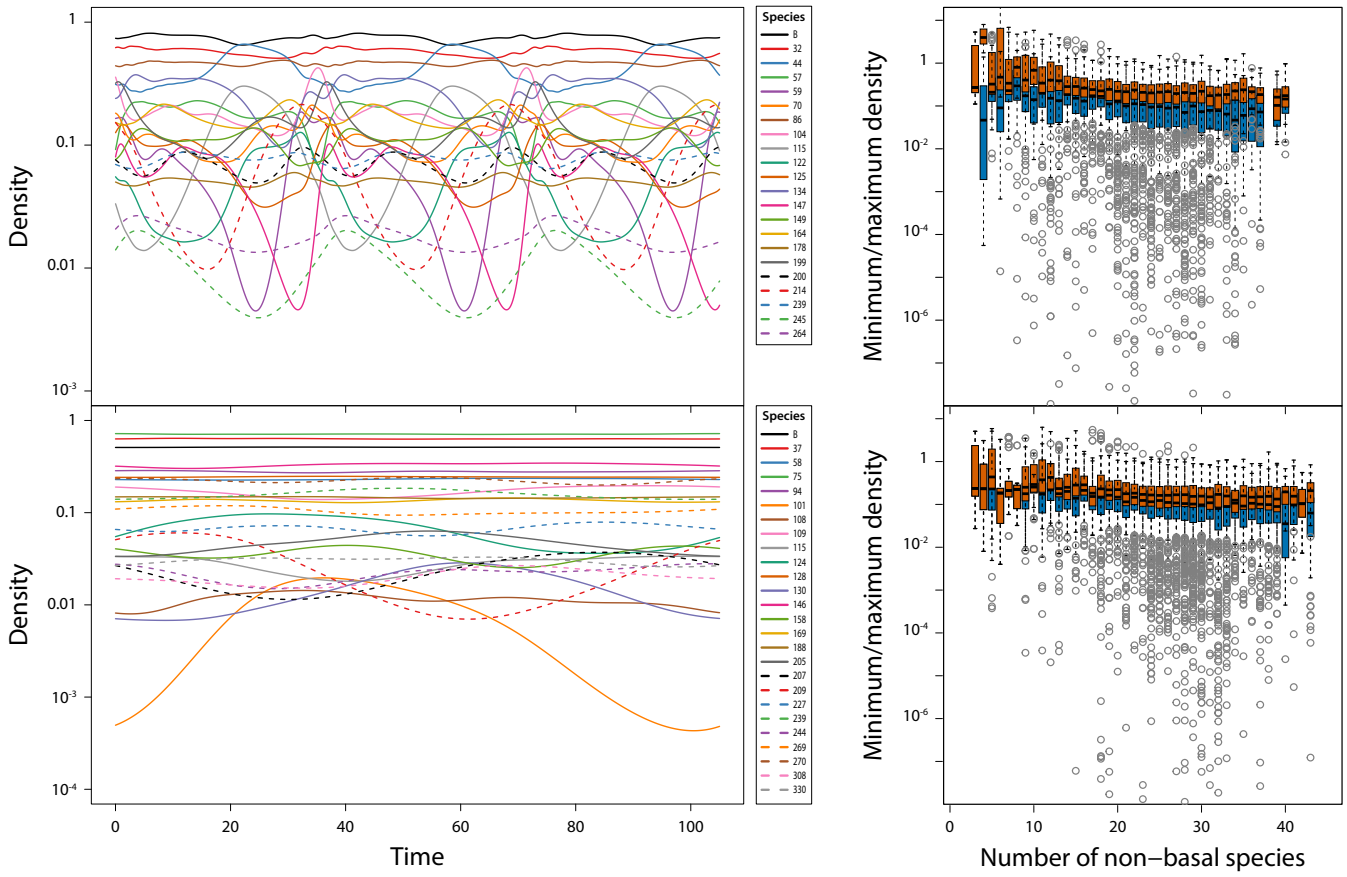

Fig. S9. Juvenile-adult asymmetry in biomass dynamics stabilises community dynamics – *A*: Examples of total biomass dynamics of all species in food web simulations using the 3-stage biomass model including juveniles, subadults and adults (see *Stage-structured biomass model of species dynamics* above) when juveniles are more vulnerable to predation and subadults are limited most by food availability (top panel; $q = 0.9$, $\phi = 1.8$) and when subadults and adults are more vulnerable to predation and juveniles are limited most by food availability (bottom panel; $q = 1.2$, $\phi = 0.2$). Corresponding food web structures are shown in Figure S8. *B*: Boxplot of minimum (blue bars) and maximum total biomass densities (red bars) as a function of community size for all persisting species in 500 replicate food web simulations using the 3-stage biomass model including juveniles, subadults and adults (see *Stage-structured biomass model of species dynamics* above) when juveniles are more vulnerable to predation and subadults are limited most by food availability (top panel; $q = 0.9$, $\phi = 1.8$) and when subadults and adults are more vulnerable to predation and small juveniles and adults are limited most by food availability (bottom panel; $q = 1.2$, $\phi = 0.2$).

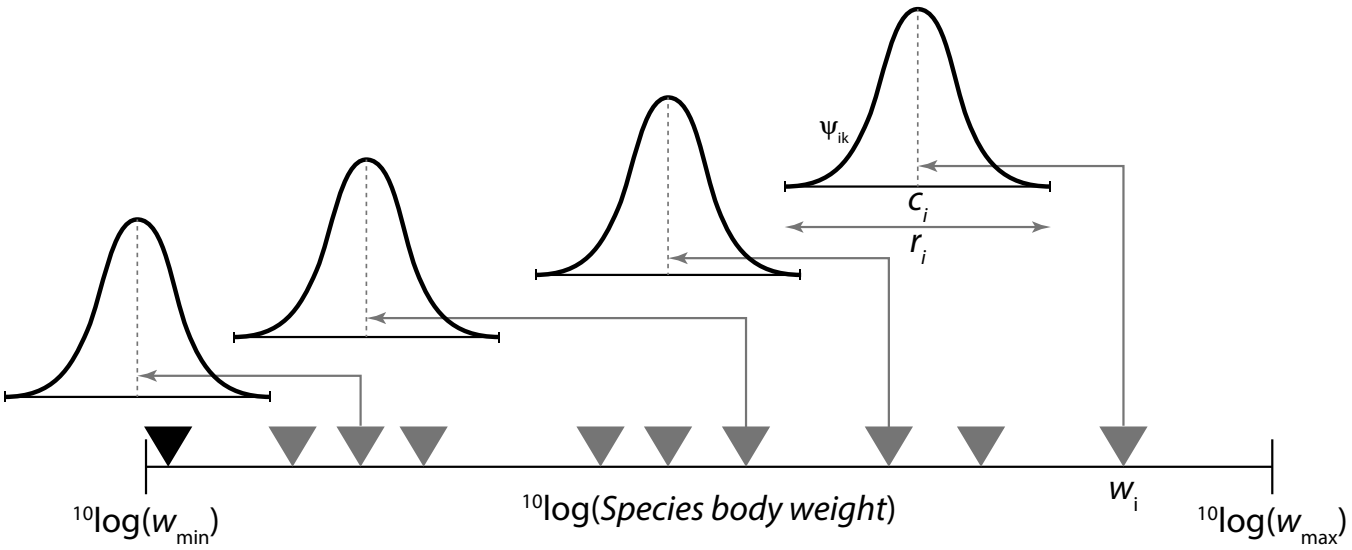

Fig. S10. Construction of the prey-predator mass ratio food web model – Species are randomly assigned niche values n_i in the range [0,1]. Niche values are related to body size w_i following $w_i = (w_{max})^{n_i}(w_{min})^{1-n_i}$ with minimum (w_{min}) and maximum body size (w_{max}) equal to 10^{-8} and 10^4 gram, respectively. The center c_i of the feeding niche of consumer species is uniformly distributed between $n_i - 2.5/^{10}\log(w_{max}/w_{min})$ and $n_i - 0.5/^{10}\log(w_{max}/w_{min})$, yielding median prey-predator body size ratio between $10^{-2.5}$ and $10^{-0.5}$. The feeding niche width r_i equals $1/^{10}\log(w_{max}/w_{min})$. Consumer species i feeds on all prey species k with body sizes between $(w_{max})^{(c_i-r_i/2)}(w_{min})^{(1-(c_i-r_i/2))}$ and $(w_{max})^{(c_i+r_i/2)}(w_{min})^{(1-(c_i+r_i/2))}$ at a relative feeding rate ψ_{ik} following a hump-shaped distribution of prey body size (see Materials and Methods).

References

1. Karline Soetaert. *rootSolve: Nonlinear root finding, equilibrium and steady-state analysis of ordinary differential equations*, 2009. R package 1.6.
2. Karline Soetaert and Peter M.J. Herman. *A Practical Guide to Ecological Modelling. Using R as a Simulation Platform*. Springer, Dordrecht, The Netherlands, 2009. ISBN 978-1-4020-8623-6.
3. R Core Team. *R: A language and environment for statistical computing*. R Foundation for Statistical Computing, Vienna, Austria, 2020.
4. A M de Roos, T Schellekens, T Van Kooten, K E Van De Wolfshaar, D Claessen, and L Persson. Food-dependent growth leads to overcompensation in stage-specific biomass when mortality increases: The influence of maturation versus reproduction regulation. *American Naturalist*, 170:E59–E76, 2007.
5. A M de Roos, T Schellekens, T Van Kooten, K E Van De Wolfshaar, D Claessen, and L Persson. Simplifying a physiologically structured population model to a stage-structured biomass model. *Theoretical Population Biology*, 73(1):47–62, 2008.
6. A M de Roos and L Persson. *Population and community ecology of ontogenetic development*. Monographs in Population Biology 51. Princeton University Press, Princeton, NJ, 2013.